Science Translational Medicine
AAAS

stm.sciencemag.org/cgi/content/full/12/564/eaay4799/DC1

Supplementary Materials for

ICOSL$^+$ plasmacytoid dendritic cells as inducer of graft-versus-host disease, responsive to a dual ICOS/CD28 antagonist

Djamilatou Adom, Stacey R. Dillon*, Jinfeng Yang, Hao Liu, Abdulraouf Ramadan, Kushi Kushekhar, Samantha Hund, Amanda Albright, Maykala Kirksey, Titilayo Adeniyan, Katherine E. Lewis, Lawrence Evans, Rebecca Wu, Steven D. Levin, Sherri Mudri, Jing Yang, Erika Rickel, Michelle Seaberg, Katherine Henderson, Chelsea J. Gudgeon, Martin F. Wolfson, Ryan M. Swanson, Kristine M. Swiderek, Stanford L. Peng, Keli L. Hippen, Bruce R. Blazar, Sophie Paczesny*

*Corresponding author. Email: paczesns@musc.edu (S.P.); stacey.dillon@alpineimmunesciences.com (S.R.D.)

Published 7 October 2020, *Sci. Transl. Med.* **12**, eaay4799 (2020)
DOI: 10.1126/scitranslmed.aay4799

The PDF file includes:

Other Supplementary Material for this manuscript includes the following:

(available at stm.sciencemag.org/cgi/content/full/12/564/eaay4799/DC1)

Materials and Methods

Generation of ALPN-101 using the vIgD platform

The Variant Immunoglobulin Domain (vIgD) platform (*21*) uses yeast display and reiterative flow cytometry-based screening to create therapeutically applicable protein domains with tailored specificity and affinity, with 'vIgDs' created through directed evolution of naturally occurring proteins such as immunoglobulin superfamily (IgSF) members like ICOSL. ALPN-101 (ICOSL vIgD-Fc) (**Fig. 3A**) was created on this platform by evolving a human ICOSL extracellular domain toward improved binding to ICOS as well as high-affinity binding to CD28, a target which is not appreciably bound by wild-type (WT) ICOSL. The therapeutic candidate ALPN-101 is a dimer of the platform-matured ICOSL vIgD domain fused to a modified IgG1 lacking FcγR (CD16a, CD32, and CD64) or C1q binding, but retaining FcRn binding, resulting in a dual human ICOS/CD28 inhibitor. Flow-based binding assays demonstrated high-affinity binding of ALPN-101 to both ICOS and CD28; the ICOSL domain used to generate ALPN-101 was isolated after just the 2nd round of selection. To calculate EC_{50} values for ALPN-101 binding to its targets, Expi293 cells (ThermoFisher Scientific) were transfected with expression plasmids encoding human CD28, ICOS, or CTLA-4, and the cells were incubated for 24 hours at 37°C/5% CO_2 with shaking. On the following day, transiently transfected Expi293 cells were harvested, counted, and adjusted to a concentration of 5 x 10^6 cells/mL in PBS. A 1:1000 dilution of NEAR-IR Live/Dead dye was added and the cells were incubated for 15 min at room temperature, washed in FACS buffer (PBS, 0.5% BSA, 0.1% NaN_3, 0.5 mM EDTA), adjusted to 1 x 10^6 cells/mL, mixed with ALPN-101 (serially diluted 1:5 starting at 100 nM in FACS buffer) or other test articles, and incubated for 45 min at RT. Cells were then washed and stained with goat anti-human IgG PE (Jackson ImmunoResearch) to detect bound protein. After a 30 min incubation at RT, cells were washed twice and analyzed on an LSR II flow cytometer (Becton Dickinson), and data analysis was performed using FlowJo software. To assess the target specificity of ALPN-101, it was tested for binding to a panel of 17 human IgSF proteins expressed during transient transfection in HEK-293 cells (Gibco). ALPN-101 bound CD28, ICOS, and CTLA-4 specifically and in a dose-dependent manner, while no binding was observed to the other cell surface-expressed IgSF proteins evaluated (BTLA, CD96, CD112R, CD155, CD160, CD226, NECL1, NECL2, NECL3, NECL4, PD-L1, PVRL1, PVRL2, PVRL3, PVRL4, TIGIT, or TMIGD2).

Test Articles

Nulojix (belatacept) and Orencia (abatacept) were purchased from Catalent, and anti-ICOSL mAb (prezalumab) was purchased from Creative Biolabs. ALPN-101 was produced at KBI Biopharma. The WT ICOSL-Fc, matched Fc control, anti-CD28 (knob-into-hole heterodimeric Fc fusion protein using a single Fab derived from an anti-CD28-binding antibody (US patent no. 8,785,604 B2), and anti-ICOS (using Fab domains derived from vopratelimab/JTX-2011; http://www.imgt.org/3Dstructure-DB/cgi/details.cgi?pdbcode=10730), all containing the same Fc sequence as ALPN-101, were produced at Alpine Immune Sciences (AIS).

Jurkat assay for functional characterization of ALPN-101. Human Jurkat T cells expressing endogenous CD28, an IL-2-luciferase reporter gene, and a transfected chimeric ICOS/CD28 molecule (the ICOS extracellular domain fused to the intracellular tail of CD28) were stimulated with plate-bound WT ICOSL-Fc or WT CD86-Fc (AIS) in the presence or absence of titrated amounts (4-fold dilutions from 0.001-300 nM) of ALPN-101, belatacept/abatacept (Catalent), anti-ICOSL mAb (Creative Biolabs), or Fc control (AIS). The % inhibition of the luciferase signal in the presence of various concentrations of the test articles [defined as (1 – experimental value/mean value of Fc control wells) x 100] was plotted vs. the log transform of test article concentration (nM).

Generation of Artificial Antigen Presenting Cells (aAPCs) and Effector Cells

Artificial APCs (aAPCs) were generated by transducing K562 cells (ATCC CCL-243) with lentivirus to express cell surface anti-human CD3 single chain variable fragment (OKT3 scFv) and full-length, human CD80, CD86, and/or ICOSL (K562/OKT3/CD80, CD86, ICOSL, or CD80/CD86/ICOSL). Cells were selected with puromycin, and surface expression of the transgenes was confirmed by flow cytometry. Cells were cultured in complete RPMI medium (RPMI 1640 (Life Technologies) supplemented with 10% FBS (VWR), 1X NEAA (Life Technologies), 1X GlutaMAX (Life Technologies), 1X penicillin-streptomycin (VWR), 1 mM sodium pyruvate (Life Technologies)) at 37°C with 5% CO_2. For effector cells, Jurkat/IL-2 cells expressing endogenous CD28 and luciferase driven by an IL-2 promoter were purchased from Promega. An ICOS-CD28 chimeric receptor composed of the extracellular domain (ECD) and transmembrane domain (TM) of ICOS and the intracellular domain (ICD) of CD28 was transduced into the Jurkat/IL-2 cells (Jurkat/IL-2/ICOS-CD28; fig. S13B) to provide luminescent signal upon ICOSL - ICOS interaction. Cells were cultured in complete RPMI with 1 mg/mL hygromycin.

Bioassay of CD80/CD86 – CD28 or ICOSL – ICOS Blockade

APCs were added at 2.5x10^4 cell per well in 33 µL Jurkat Assay Buffer (RPMI 1640 + 5% FBS). ALPN-101 or comparators were diluted from stock solutions and titrated. Titrated proteins were added at 33 µL per well and incubated with aAPCs for

15 – 30 minutes at room temperature with shaking. Jurkat/IL-2 or ICOS-CD28 cells were harvested, counted, and adjusted to add $1.25x10^5$ cells per well in 33 µL media per well. Plates were incubated for 5 hours at 37°C with 5% CO_2. Assay plates developed with 100 µL per well of cell lysis and luciferase substrate solution (BioGlo luciferase reagent, Promega). Relative luminescence units (RLU) were determined for each test sample by measuring luminescence with a 1 second per well integration time using a Cytation 3 imaging reader (BioTek Instruments).

Bio-Layer Interferometry (BLI) Affinity Measurements

BLI analysis of ALPN-101 binding affinity was conducted using the Forté Bio Octet RED384 system. After a 120-second baseline to confirm sensor stability, ALPN-101 was loaded onto anti-human IgG capture sensors in Forté Bio kinetic buffer at a concentration of 50 nM. To correct for non-specific binding, parallel anti-human IgG capture sensors were loaded with 50 nM of an irrelevant Fc fusion protein. After loading, another baseline reading was performed followed by association of recombinant monomeric CD28:His, ICOS:His, or CTLA-4:His proteins (all from Acro Biosystems) as well as a blank buffer sample for each titration. CD28:His was tested in a five-point, 2.5-fold titration at 30, 12, 4.8, 1.9, and 0.8 nM; ICOS:His and CTLA-4:His were tested in a five-point, 2-fold titration at 20, 10, 5, 2.5, and 1.25 nM. After association, each sample was allowed to dissociate for the amount of time required to achieve at least a 10% decrease in signal, corresponding to 1500 seconds for CD28, 3600 seconds for ICOS, and 2400 seconds for CTLA-4. After the data were acquired, the reference sensor signal and blank buffer sample signal were subtracted from each titration and the curves were globally fit with a 1:1 model to determine the k_a and k_d of each counter structure. The errors of the association and dissociation were calculated along with the K_D and full R^2. Results presented are from three independent experiments.

Mixed Lymphocyte Reactions (MLRs)

To evaluate the effects of ALPN-101 on the proliferation of primary T cells (**Figs. 3B** and fig. S13D), a human MLR was performed in presence of 200 µg/ml of ALPN-101 or control Fc fusion proteins. Pan-T cells were thawed, labeled with CFSE, washed, and mixed with monocyte-derived DCs matured with LPS generated from an unrelated donor, in the presence of 3-fold dilutions of Fc protein test articles. Plates were incubated for 4 days at 37°C with 5% CO_2. Proliferation was determined via flow cytometry by quantitating the percentage of CFSE-labeled CD4+ and CD8+ T cells diluting CFSE over time. Supernatants were tested for cytokine concentrations using a MILLIPLEX MAP Human Cytokine/Chemokine Magnetic Bead Panel multiplex assay (HCYTOMAG-60K, including beads specific for human IFNγ, IL-2, IL-13, IL-17A, GM-CSF, and TNFα), from EMD Millipore. Samples were assayed according to the manufacturer's protocol, and then analyzed on a MAGPIX instrument (EMD Millipore). Data analysis was performed using xPONENT 4.2 software.

Isolation of Intestinal Cells

Single-cell suspensions were prepared from intestines as described previously (*23*). Briefly, intestines were flushed with phosphate-buffered saline (PBS) to remove fecal matter and mucus. Fragments (<0.5 cm) of intestines were digested in 10 ml DMEM containing collagenase type B (2 mg/mL; Roche), deoxyribonuclease I (10 µg/mL; Roche), and 4% bovine serum albumin (Sigma-Aldrich) at 37°C with shaking for 90 min. The digested mixture was then diluted with 30 ml plain DMEM, filtered through a 70-µm strainer and centrifuged at 850 *g* for 10 min. The cell pellets were suspended in 5 ml of 80% Percoll (GE Healthcare), overlaid with 8 ml of 40% Percoll, and centrifuged at 2000 rpm for 20 min at 4°C without braking. Enriched lymphocytes were collected from the interface.

Flow Cytometry for murine studies

Cells were pre-incubated with purified anti-mouse CD16/CD32 mAb for 10 to 20 min at 4°C to prevent nonspecific binding of the antibodies. The cells were subsequently incubated for 30 min at 4°C with antibodies for surface staining. Fixable viability dye (FVD) was used to distinguish live cells from dead cells. The FoxP3/Transcription Factor Staining Buffer Set and the Fixation and Permeabilization Kit were used for intracellular transcription factor and cytokine staining. For cytokine staining, cells were restimulated with phorbol myristate acetate (PMA; 50 ng/ml), ionomycin (1 µg/ml; Sigma-Aldrich), and brefeldin A for 4 to 6 hours before any staining. Cell surface staining of murine surface markers included antibodies specific for CD11c (clone N418), CD11b (clone M1/70), B220 (clone RA3-6B2), CD103 (clone 2EF), RORγt (clone Q31-378), IL-17 (clone TC11-18H10), and IFNγ (clone XMG1.2).

For the human PBMC-NSG GVHD model studies described in **Fig. 3,** figs. S14-16, and fig. S19, engrafted human CD45+ cells in whole blood collected from the NSG recipients were detected and their cell surface phenotype characterized by flow cytometry using an LSR II flow cytometer, and data analysis was performed using FlowJo software. Drug binding to targets was assessed by staining cells with anti-human IgG, which binds the Fc of ALPN-101 or belatacept. Cells expressing the targets of the test articles (CD28 and/or ICOS on T cells for ALPN-101 or CD80/CD86 on APC for belatacept) bind the test articles and can be detected with an anti-human IgG reagent by flow cytometry. Of note, ALPN-101 blocks the binding of all anti-CD28 and anti-ICOS flow antibodies evaluated to date, a feature that precludes the simultaneous assessment of CD28 and ICOS expression and ALPN-101 binding to cells expressing these targets. The antibodies used in these analyses were purchased from BioLegend: anti-CD4-PE-Cy5.5 (clone RPA-T4), anti-CD8-PE-Cy7 (clone RPA-T8), anti-CD45RA-BV420 (clone HI100), anti-ICOS-FITC (clone C398.4A), anti-CD28-PE-Texas Red (clone CD28.2), anti-PD-1-BV605 (clone

EH12.2H7), and anti-human IgG-APC-H7 (clone HP6017), anti-PD-1-APC (clone EH12.2H7), anti-Ki67-BV510 (clone Ki-67), anti-CD20-PerCP-Cy5.5 (clone 2H7), anti-CD14-FITC (clone 63D3), anti-FoxP3-Pacific Blue (clone 259D), anti-CD45-PerCP-Cy5.5 (clone HI30), anti-ICOS-AF700 (clone BB7.2), anti-human IgG-PE (clone HP6017), anti-CD8-PE (clone SK1), anti-CD28-PE-Cy7 (clone CD28.2), anti-CD4-BV711 (clone RPA-T4), anti-CD8-BV650 (clone RPA-T8), anti-CD95-FITC (clone DX2), anti-CD56-APC (clone 5.1H11), anti-CD3-BV510 (clone OKT3), anti-CD25-PerCP-Cy5.5 (clone M-A251), anti-CD27-BV605 (clone O323), anti-CD27-FITC (clone M-T271), anti-CD25-BV605 (clone BC96), and anti-CD16-BV711(clone 3G8). Anti-CD4-eFluor 450 (clone OKT4) was purchased from Thermo Fisher Scientific.

For the study described in **Figs**. **5D-J** and **6** using immunocompromised models, we used hCD45 (clone 2D1) and the same human antibodies used for analysis of the patient cohort.

For the flow binding assessments described in fig. S15 $4x10^5$ Jurkat/IL-2 or Jurkat/IL-2/ICOS-CD28 cells per well were plated in a 96-well, U-bottom plate. Cells were pelleted, buffer was removed, and cells suspended in titrated Fc fusion protein test articles (400,000 – 5 pM). Test articles were allowed to bind for 30 min at room temperature with shaking. Cells were washed twice with 200 µL (final) FACS buffer (PBS + 0.5% BSA + 0.05% NaN_3). Secondary anti-human IgG-APC (Jackson ImmunoResearch) was added at 0.3 µL in 50 µL per well. Samples were incubated and washed, and after the final wash, cells were fixed with 2% paraformaldehyde until analysis on an LSRII flow cytometer (BD Biosciences).

Cell Sorting. pDCs defined as $CD11b^-CD11c^+B220^+CD103^+$ and $CD4^+$ conventional T cells (T_{convs}) $Foxp3^-$ (non-Foxp3-expressing $CD4^+$ T cells, in other words non-T_{regs}) cells were sorted from the gut of C57BL/6 WT BM or $ICOSL^{-/-}$ BM recipient mice receiving allo-HCT at Day 10 post-allogeneic transplantation. Cell sorting was performed using a BD FACSAria (BD Bioscience) using sorted pDCs and CD4+ T_{convs} (purity >95%).

Nanostring Analysis. Sorted intestinal pDCs and $CD4^+$ T_{conv} $Foxp3^-$ cells from C57BL/6 WT BM or $ICOSL^{-/-}$ BM recipient aGVHD mice were directly lysed in RLT buffer (Qiagen) on ice. The cell concentration for lysis was 0.2×10^4 to 1×10^4 cells/µL in a total volume of 5 µL with RLT buffer. Lysed samples were immediately frozen in liquid nitrogen and then stored at −80°C or on dry ice. Nanostring analysis was performed with the nCounter Analysis System at NanoString Technologies. The nCounter Mouse Immunology Kit, which includes 561 immunology-related mouse genes, was used in the study. Data shown as $\log_2$ transformed ratio of fold change between cells sorted from $ICOSL^{-/-}$ and WT mice.

Enzyme-Linked Immunosorbent Assay (ELISA)
Concentrations of murine and human FLT3L in plasma were measured with the Quantikine ELISA Kit (R&D).

Pharmacokinetics Analysis
The concentration of ALPN-101 (or belatacept) was measured in the serum samples described in **Fig. 3E-F** using an ELISA method developed at Alpine Immune Sciences. ALPN-101 was captured by mouse anti-huICOSL mAb (clone MIH12; eBioscience) immobilized onto a 96-well microtiter plate and detected with Fc-specific, mouse anti-huIgG:HRP (Jackson ImmunoResearch). Belatacept was captured by mouse anti-human CTLA4 clone A3.6B10.G1 (BioLegend), and detected with the same Fc-specific, mouse anti-huIgG:HRP reagent. A calibration curve was generated for each assay plate using SoftMax Pro data acquisition and analysis software (version 6.5, Molecular Devices). A 4-parameter logistic model, without weighting, was used to fit the curve to the mean OD data and nominal concentration values at each calibrator level. The sample OD data and resulting curve fit equation were used to back-calculate test article concentrations in the study samples. Serum PK data were imported into Phoenix WinNonlin v6.4 (Certara) for analysis. To analyze the single dose ALPN-101 data, a standard noncompartmental model with extravascular administration was used to estimate PK parameters based on the group mean concentration versus time data. Nominal sample collection times were used for the calculations. Time was changed from units of hours to units of days and concentrations were changed from units of ng/mL to units of µg/mL before analysis. Analyte concentrations that were below the lower limit of quantitation (<LLOQ) were treated as missing. The following parameters were estimated: T_{max} (time of maximum observed serum concentration), C_{max} (maximum observed serum concentration), AUC_{0-t} (area under the serum concentration-time curve from time zero to the timepoint with the last measurable concentration), and $t_{1/2}$ (terminal half-life). AUC_{0-t} values were estimated using the linear up/log down trapezoidal method.

Serum Cytokine Analysis
Serum samples from human PBMC-reconstituted NSG mice (fig. S14 and table S6) were thawed, vortexed, and centrifuged at 14,000 rpm, 4°C for 5 minutes before conducting assays. Cytokines were measured using a MILLIPLEX MAP Human Cytokine/Chemokine Magnetic Bead Panel multiplex assay (HCYTOMAG-60K, including beads specific for human IFNγ, IL-1β, IL-2, IL-4, IL-5, IL-6, IL-8, IL-10, IL-12p70, IL-13, IL-17A, and TNFα), from EMD Millipore. Samples were diluted as needed (1:2 or 1:3) in the manufacturer's assay diluent and assayed in duplicate according to the manufacturer's protocol, and then analyzed on a MAGPIX instrument (EMD Millipore). Data analysis was performed with xPONENT 4.2 software.

T_{reg} proliferation and suppression assays. Human $CD4^+CD25^-$ (T_{eff}) and $CD4^+CD25^+$ (T_{reg}) T cells were purified from healthy donor PBMC (Bloodworks Northwest) via CD4 negative selection followed by CD25 positive selection and then stained with anti-FoxP3, -CD4, -PD-1, -CD25, -CD28, -CD127, -ICOS (clones noted above), as well as anti-PD-L1 (clone 29E.2A3), and anti-Helios (clone 22F6) antibodies (Biolegend), to confirm their enrichment and surface phenotype before culture (**Fig. 4A-C**). Enriched T_{reg} cells were labeled with CellTrace Violet (CTV; Thermo Fisher) and cultured with 1 µg/mL soluble anti-CD3 (clone OKT3) Ab, 50 IU/mL rIL-2, and mitomycin C-treated CD80-transfected K562 antigen-presenting cells (to provide a strong co-stimulatory signal and present the anti-CD3 Ab to T_{reg} cells via FcR), in medium alone or with various concentrations of the test articles: Fc control, belatacept, or ALPN-101. After a 3-day incubation at 37°C, the extent of proliferation of the T_{reg} cells was assessed by CTV dilution via flow cytometry on an LSR II cytometer. T_{reg} cells labeled with CTV were mixed at various ratios with T_{eff} cells labeled with CFSE and cultured with mitomycin C-treated K562 antigen-presenting cells (which express low amounts of endogenous CD80), 60 ng/mL soluble anti-CD3 Ab, and 30 nM of each test article. Proliferation of the T_{eff} cells after a 4-day incubation at 37°C was assessed by CFSE dilution via flow cytometry. Specific T_{reg} suppression activity was calculated as follows: % suppression = (1-(Test/Control)) x 100, where Test= T_{eff} proliferation with T_{reg} and test article, and Control= T_{eff} proliferation with test article but without T_{reg}. This allowed quantification of the effects of T_{reg} on T_{eff} proliferation, independent of the effects of each test article on T_{eff}.

Stimulation of pDCs with CpG and FLT3L

Freshly isolated healthy donor PBMCs were used for the enrichment of pDCs using the human Plasmacytoid Dendritic Cell isolation kit (Miltenyi). Purity of enriched pDCs was then verified using flow cytometry, and enriched pDCs with purity ≥ 99% were subsequently plated into a 96-well with or without 0.25 µM CpG +/- 200 ng/ml FLT3L overnight. Stimulation of $ICOSL^+$ pDCs was verified using flow cytometry before transplant.

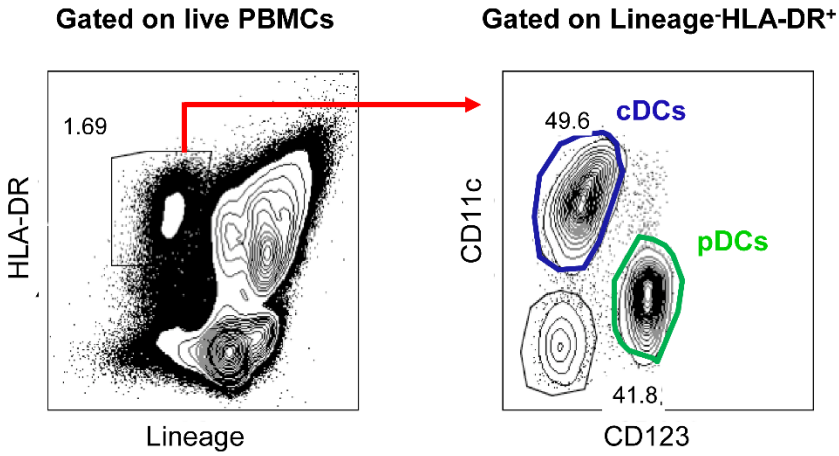

Fig. S1. pDCs and cDCs gating strategy. pDCs are defined as Lin-HLA-DR+CD123+CD11c-; cDCs are defined as Lin-HLA-DR+CD123-CD11c+. Lin, lineage.

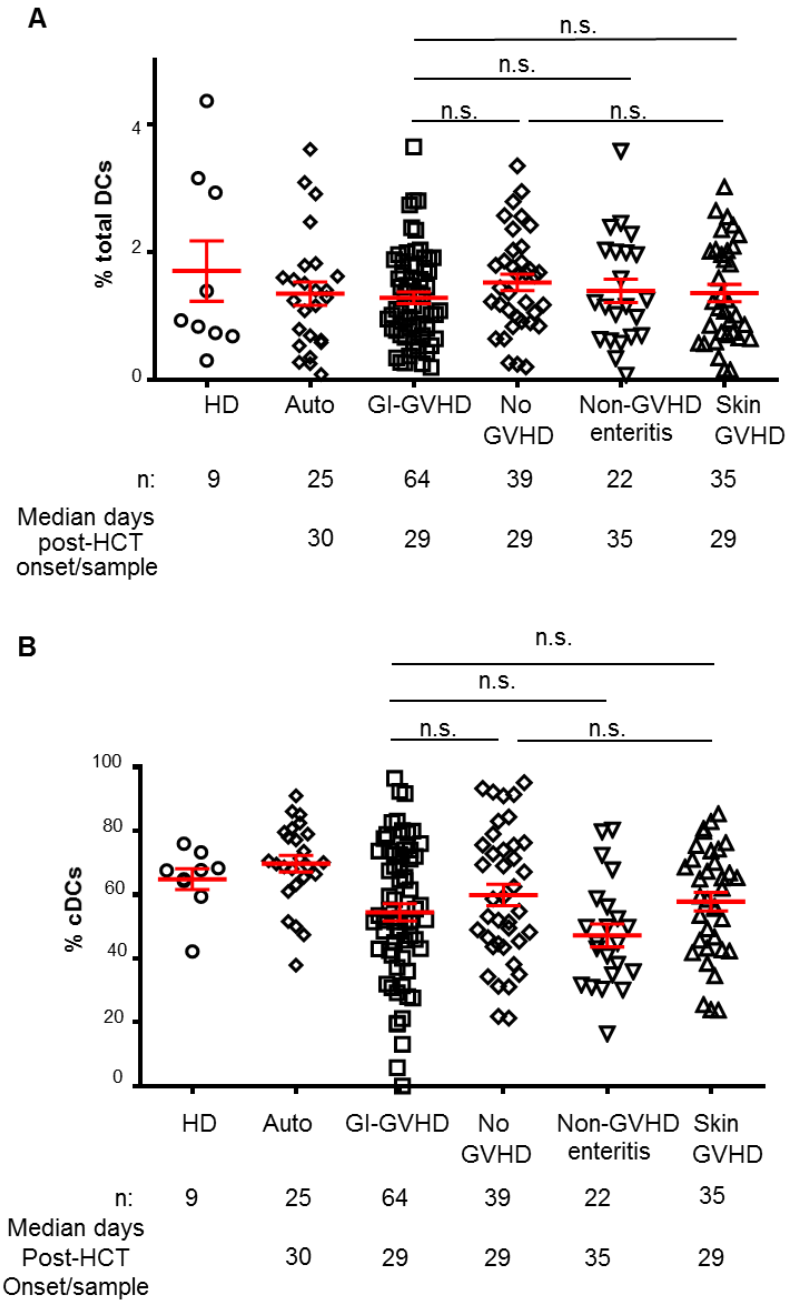

Fig. S2. Frequencies of total DCs and cDCs in patient cohort. The percentage of **(A)** total DCs and **(B)** cDCs in healthy donors (HD), patients receiving autologous HCT (Auto), and patients receiving allogenic HCT with the indicated complications. Data are shown as mean ± SEM, and statistical significance was determined using an unpaired t-test. n is number of patients. Median days indicates the median time after HCT or after onset of symptoms that samples were collected.

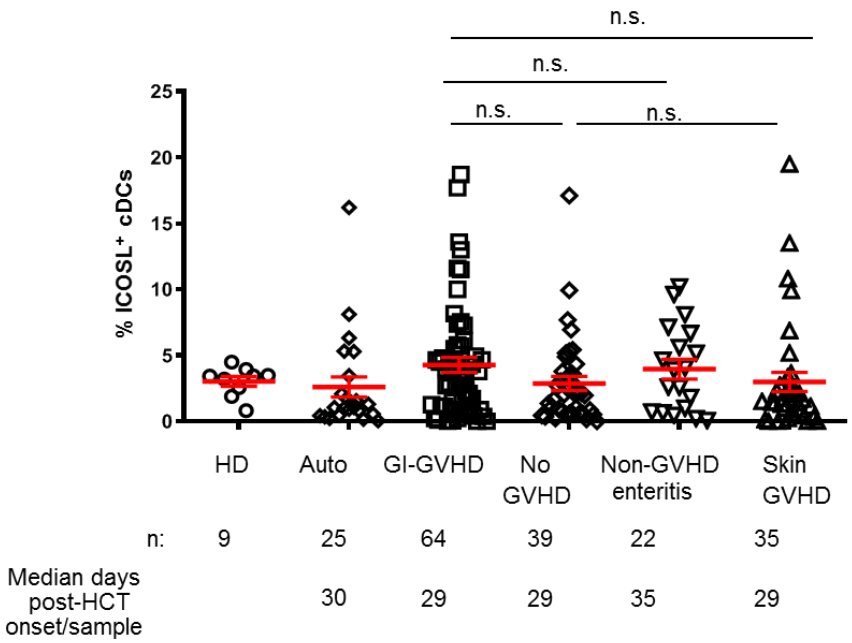

Fig. S3. Frequencies of ICOSL$^+$ cDCs in patient cohort. The percentage of ICOSL$^+$ cDCs in healthy donors (HD), patients receiving autologous HCT (Auto), and patients receiving allogenic HCT with the indicated complications. Data are shown as mean ± SEM, and statistical significance was determined using an unpaired t-test.

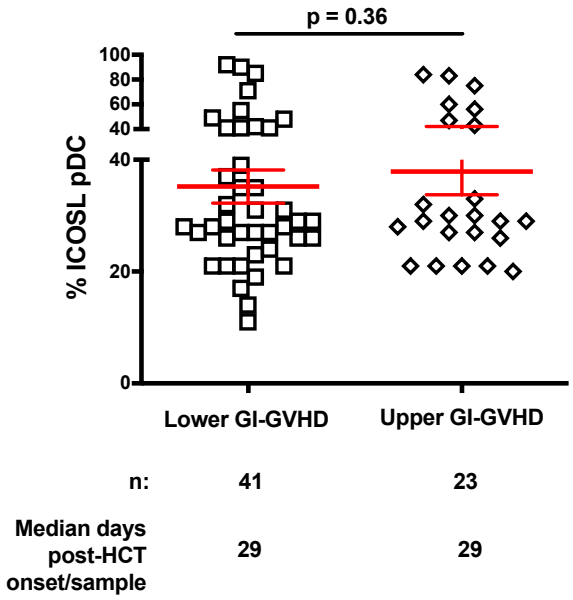

Fig. S4. Frequencies of ICOSL$^+$ pDCs in lower and upper GI-GVHD. The percentage of ICOSL$^+$ pDCs in 41 patients with lower GI-GVHD was compared to 23 patients with upper GI-GVHD. Data are shown as mean ± SEM, and statistical significance was determined using an unpaired t-test.

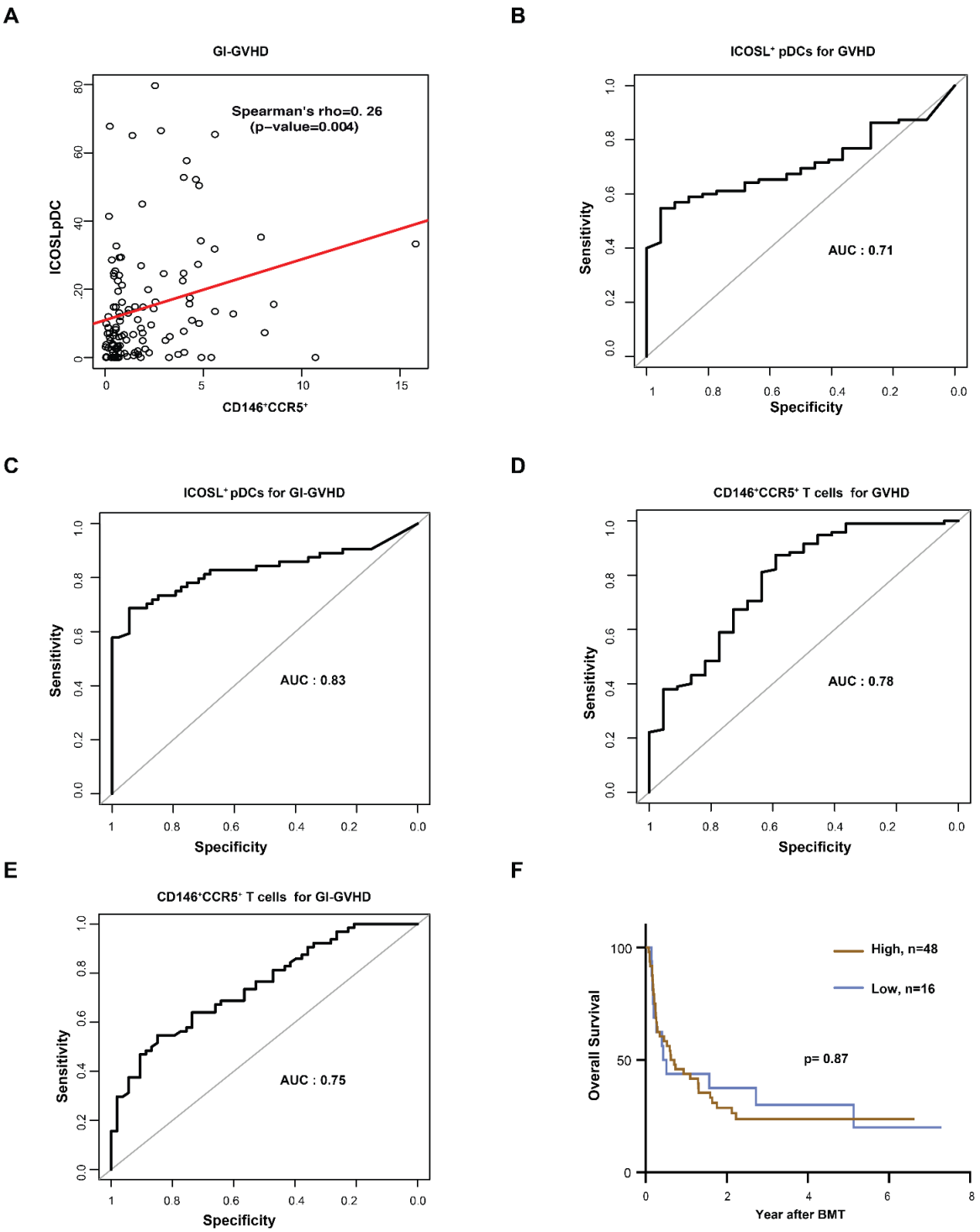

Fig. S5. Correlative and ROC analyses in patients with GVHD and GI-GVHD. (A) ICOSL$^+$ pDCs and CD146$^+$CCR5$^+$ correlation in GI-GVHD patients. (**B, C)** ROC of ICOSL$^+$ pDCs for all patients with GVHD (B) and those with GI-GVHD (C). (**D, E)** ROC CD146$^+$CCR5$^+$ for all patients with GVHD (D) and those with GI-GVHD (E). **(F)** Overall survival among patients with GI-GVHD according to high or low frequency of ICOSL$^+$ pDCs; 48 patients were in the high frequency group and 16 were in the low frequency group.

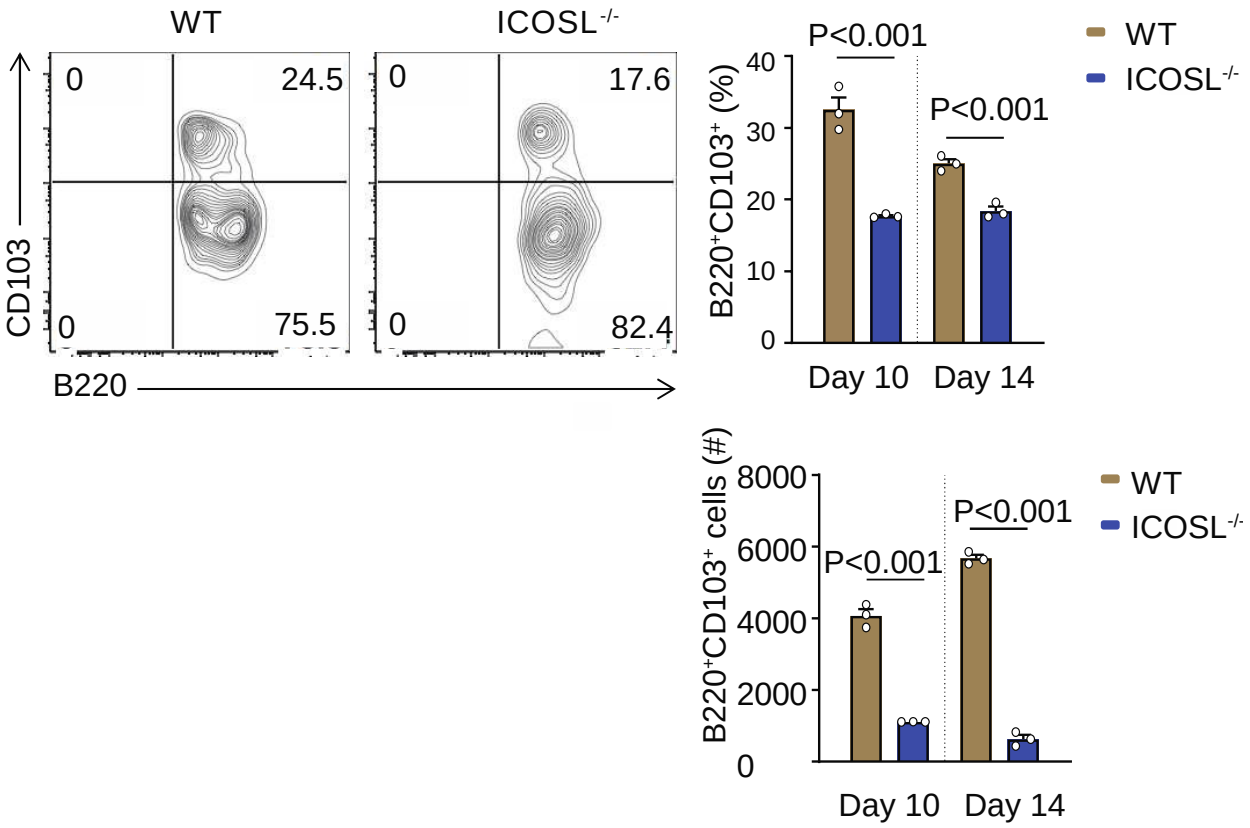

Fig. S6. Frequencies and absolute counts of murine CD11b^{-}CD11c^{+}CD103^{+}B220^{+} splenic pDCs in a major mismatch model. BALB/c mice were sublethally irradiated at 900 cGy, and then injected IV with 1×10^{6} of WT B6 T cells and 5×10^{6} of BM cells from WT or ICOSL$^{-/-}$ donor mice. CD11b^{-}CD11c^{+}CD103^{+}B220^{+} pDCs from the spleens of WT and ICOSL$^{-/-}$ BM recipient mice harvested at Day 10 and 14 post-HCT (n=3). Data are shown as mean ± SEM, and statistical significance was determined using an unpaired t-test.

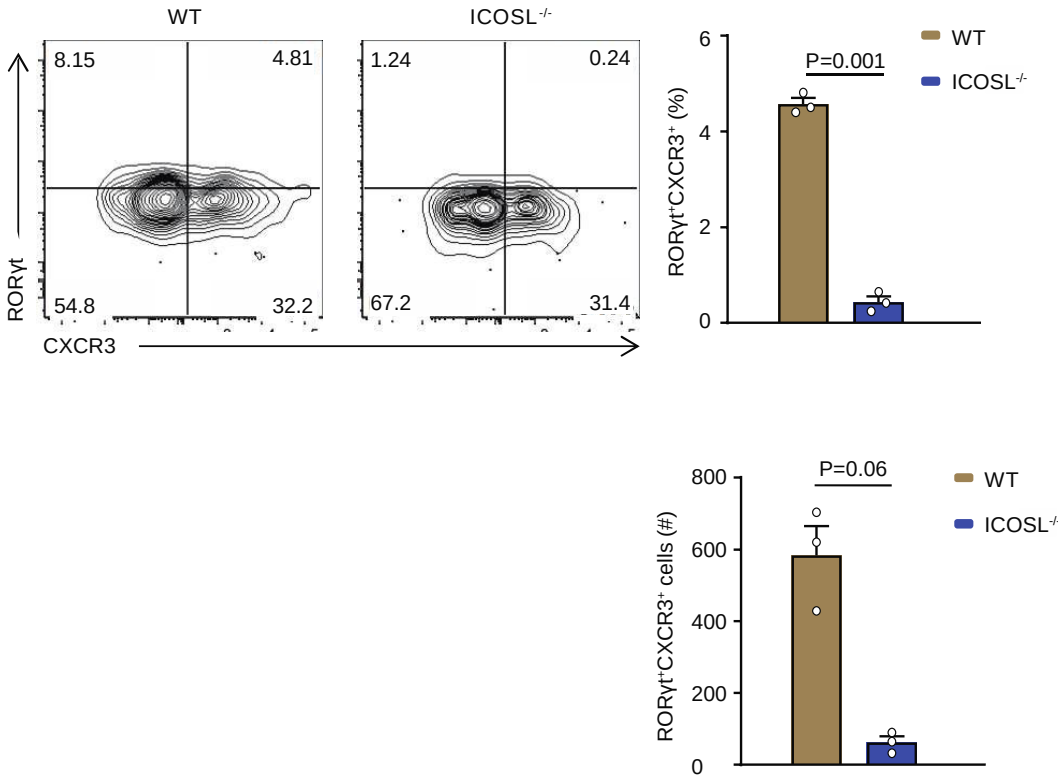

Fig. S7. Splenic Th17 cells coexpressing CXCR3 and RORγt in a major mismatch murine model. BALB/c mice were sublethally irradiated at 900 cGy, and then injected intravenously with 1×10^6 WT B6 T cells and 5×10^6 of BM cells from WT or ICOSL$^{-/-}$ donor mice. Th17 cells coexpressing RORγt and CXCR3 were detected in spleens collected at Day 10 post-HCT (n=3) of WT and ICOSL$^{-/-}$ BM recipient mice. Data are shown as mean ± SEM, and statistical significance was determined using determined using an unpaired t-test.

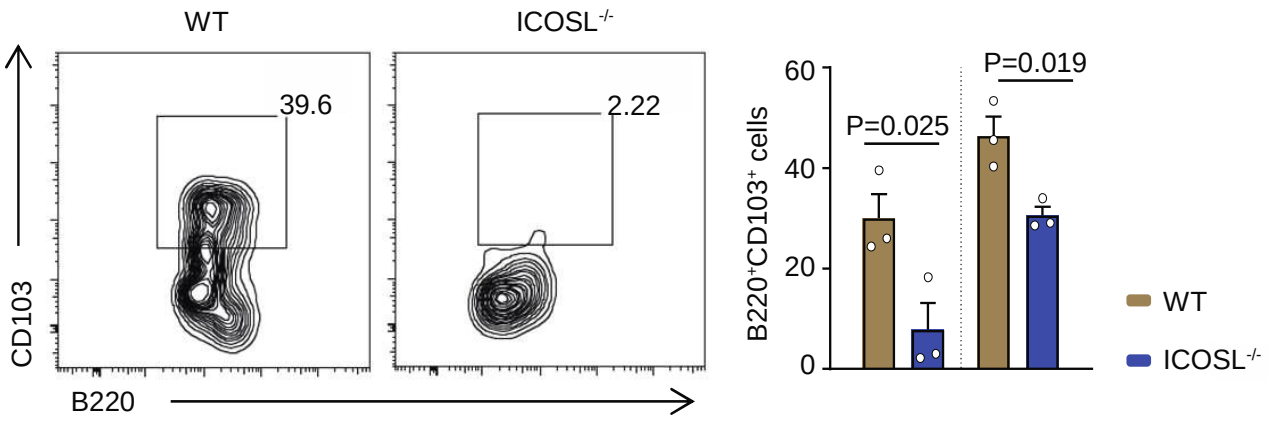

Fig. S8. Frequencies of murine intestinal CD11b^{-}CD11c^{+}CD103^{+}B220^{+} pDCs in a haploidentical allogeneic model. B6D2F1 mice were sublethally irradiated at 1000 cGy, and then injected intravenously with 2 × 10^{6} WT B6 T cells and 5 × 10^{6} BM cells from WT or ICOSL$^{-/-}$ donor mice. CD11b^{-}CD11c^{+}CD103^{+}B220^{+} pDCs were identified in the intestine of the recipient mice at Day 10 and 14 post-HCT (n=3). Data are shown as mean ± SEM, and statistical significance was determined using an unpaired t-test.

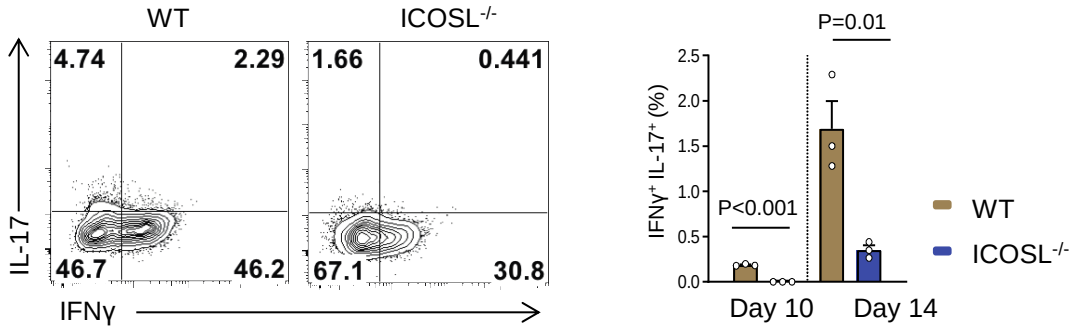

Fig. S9. Frequencies of IFNγ/IL-17–producing T cells in the gut in a haploidentical allogeneic model. B6D2F1 mice were sublethally irradiated at 1000 cGy, and then injected intravenously with 2×10^6 WT B6 T cells and 5×10^6 BM cells from WT or ICOSL$^{-/-}$ donor mice. IFNγ$^+$IL-17$^+$Th17 cells were detected in the intestine of WT and ICOSL$^{-/-}$ BM recipient mice at Day 10 and 14 (n=3). Data are shown as mean ± SEM, and statistical significance was determined using an unpaired t-test.

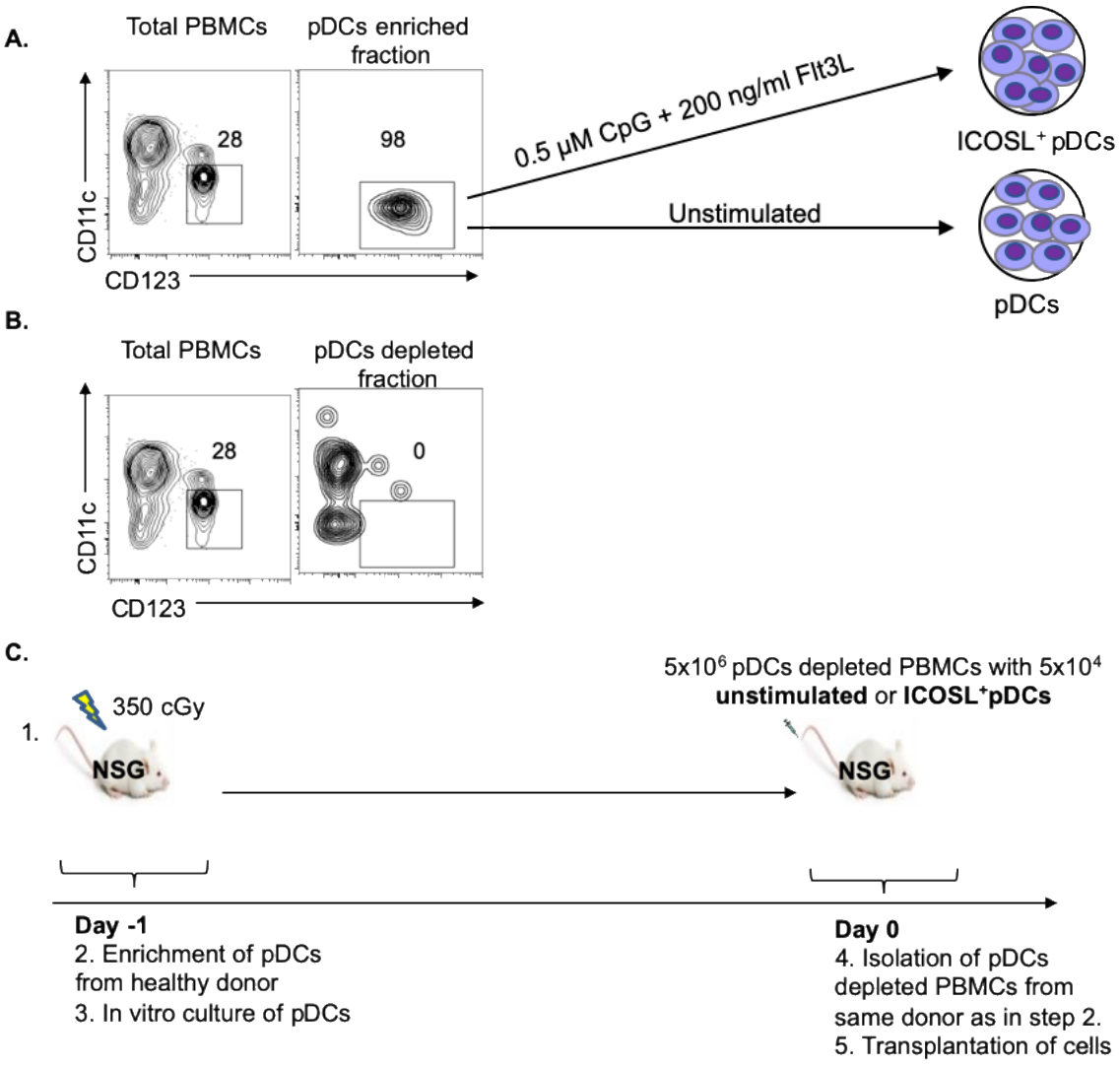

Fig. S10. Cell population pretransplant, and model of transplant. (A) PBMCs were isolated using Ficoll gradient centrifugation from a healthy human donor buffy coat. PBMCs (2×10^8) were collected and subjected to enrichment using Miltenyi pDC isolation kit. The frequency of pDCs was determine by flow cytometry in the total PBMCs and in the enriched sample. **(B**) PBMCs were isolated using Ficoll gradient centrifugation from the same healthy donor buffy coat used for pDCs enrichment. PBMCs (2×10^8) were collected and subjected to enrichment using Miltenyi pDC isolation kit. The pDC-depleted population was selected and confirmed by flow cytometry. **(C)** Timeline of experiment. On Day -1 mice were (step 1) irradiated at 350 cGy, (step 2) pDCs were enriched from human donor PBMCs and (step 3) subjected to stimulation in vitro using 0.25 µM of CpG + 200 ng/ml FLT3L or left untreated, and assessed by flow cytometry. The next day (Day 0, (step 4) pDC- depleted PBMCs were isolated from total PBMCs and (step 5) were combined with the enriched unstimulated or stimulated pDCs and the cell mixture (5×10^6 pDC-depleted PMBCs : 5×10^4 pDCs) was injected into irradiated NSG mice.

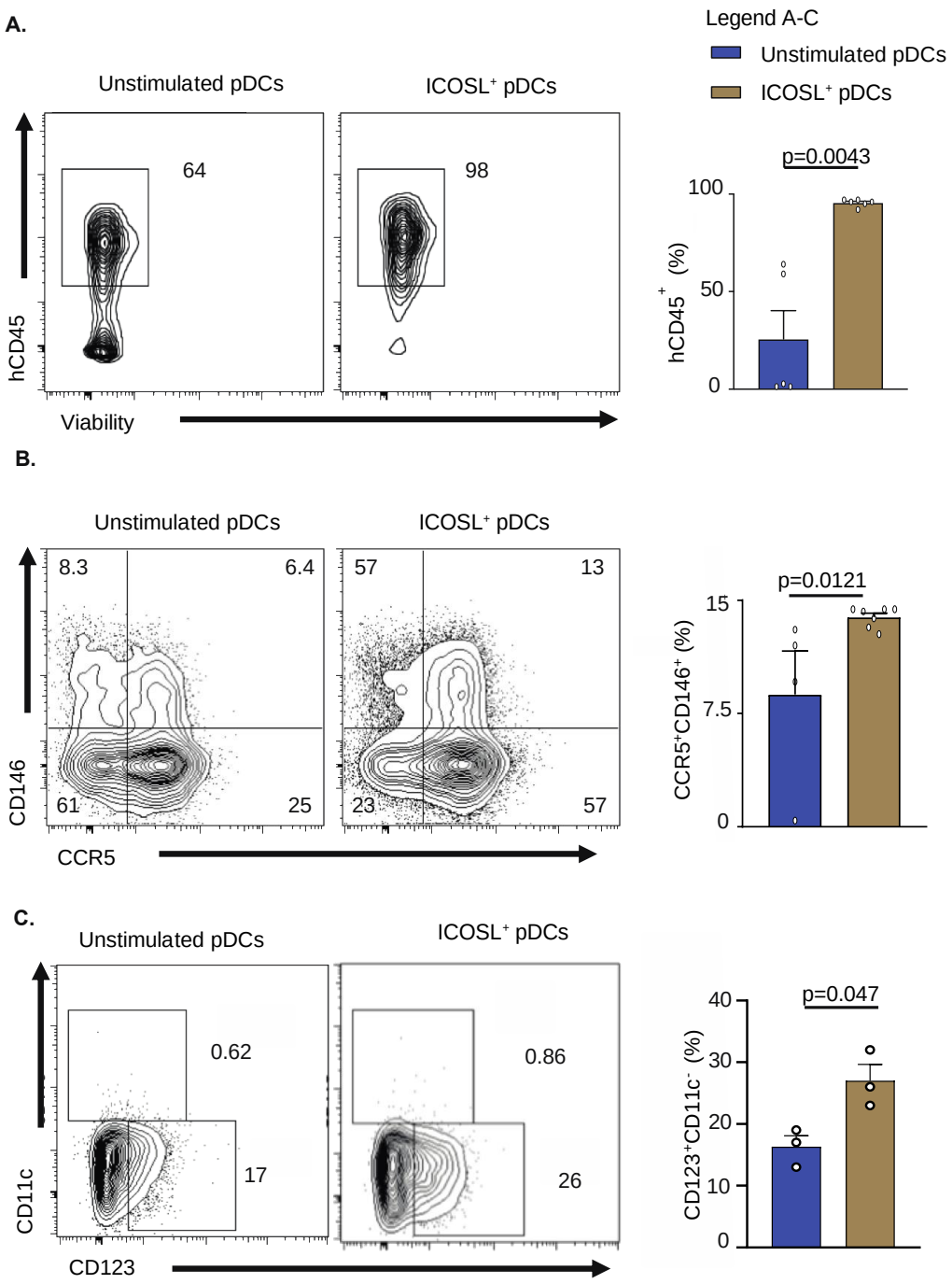

Fig. S11. Frequencies of human T cells and human pDCs in spleens of NSG mice receiving unstimulated or ICOSL$^+$ pDCs. (A) Human T cells identified with hCD45. **(B)** Human Th17 cells identified as CD146$^+$CCR5$^+$. **(C)** Human pDCs identified as Lin$^-$HLA-DR$^+$CD123$^+$CD11c$^-$. Data are shown as mean ± SEM (n = 3 or n=6), and statistical significance was determined using an unpaired t-test.

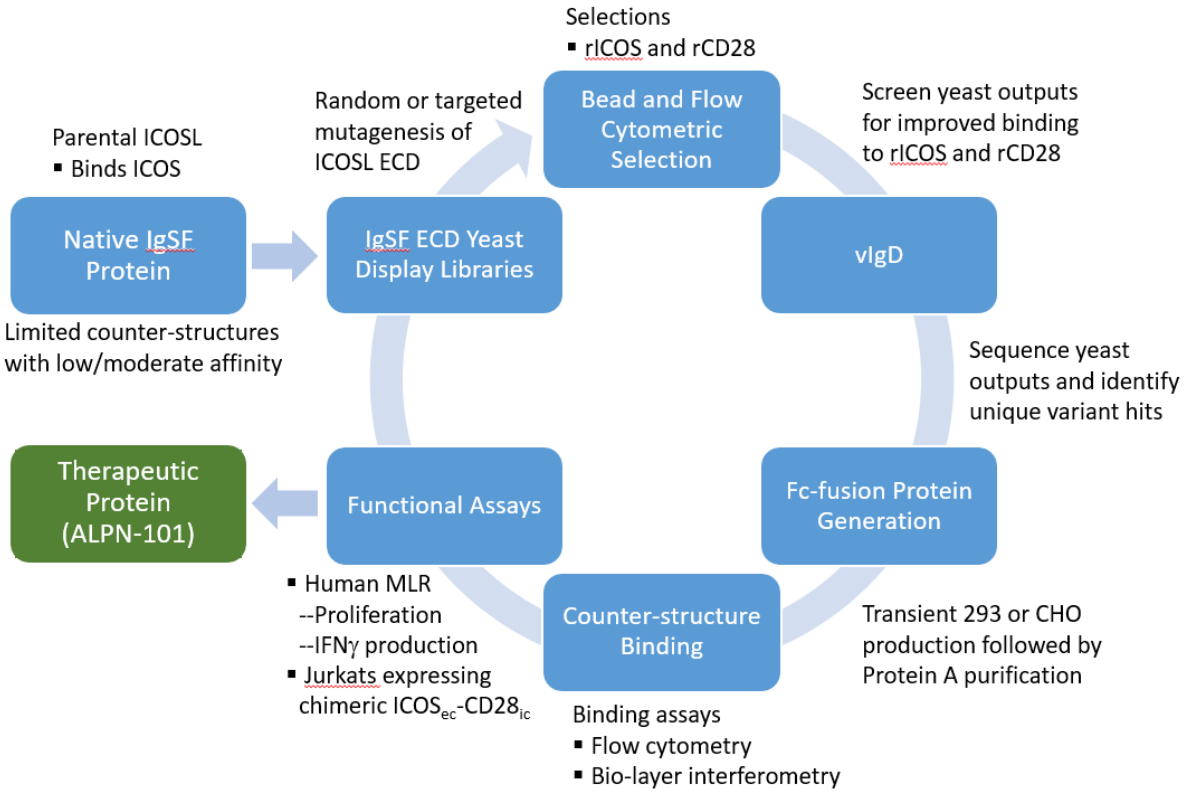

Fig. S12. Schematic of the strategy used to generate the therapeutic lead Fc fusion protein designated ALPN-101. The vIgD platform can yield yeast population outputs with increased affinity for cognate ligands or new binding partners. Repetitive selection of mutated ICOSL domains that bound to two recombinant ligands (rCD28-Fc and rICOS-Fc) resulted in yeast display of engineered ICOSL domains with increased binding towards both counter structures. ICOSL DNA sequences derived from yeast display outputs were cloned into a mammalian expression vector and produced as Fc fusion proteins in HEK-293 cells. One ICOSL vIgD domain with superior CD28 and ICOS blocking activity was selected based on functional screening results and fused to an Fc lacking FcγR (CD16a, CD32, and CD64) or C1q binding, but retaining FcRn binding, to generate the dimeric therapeutic candidate Fc fusion protein designated "ALPN-101" (**Fig. 3A**).

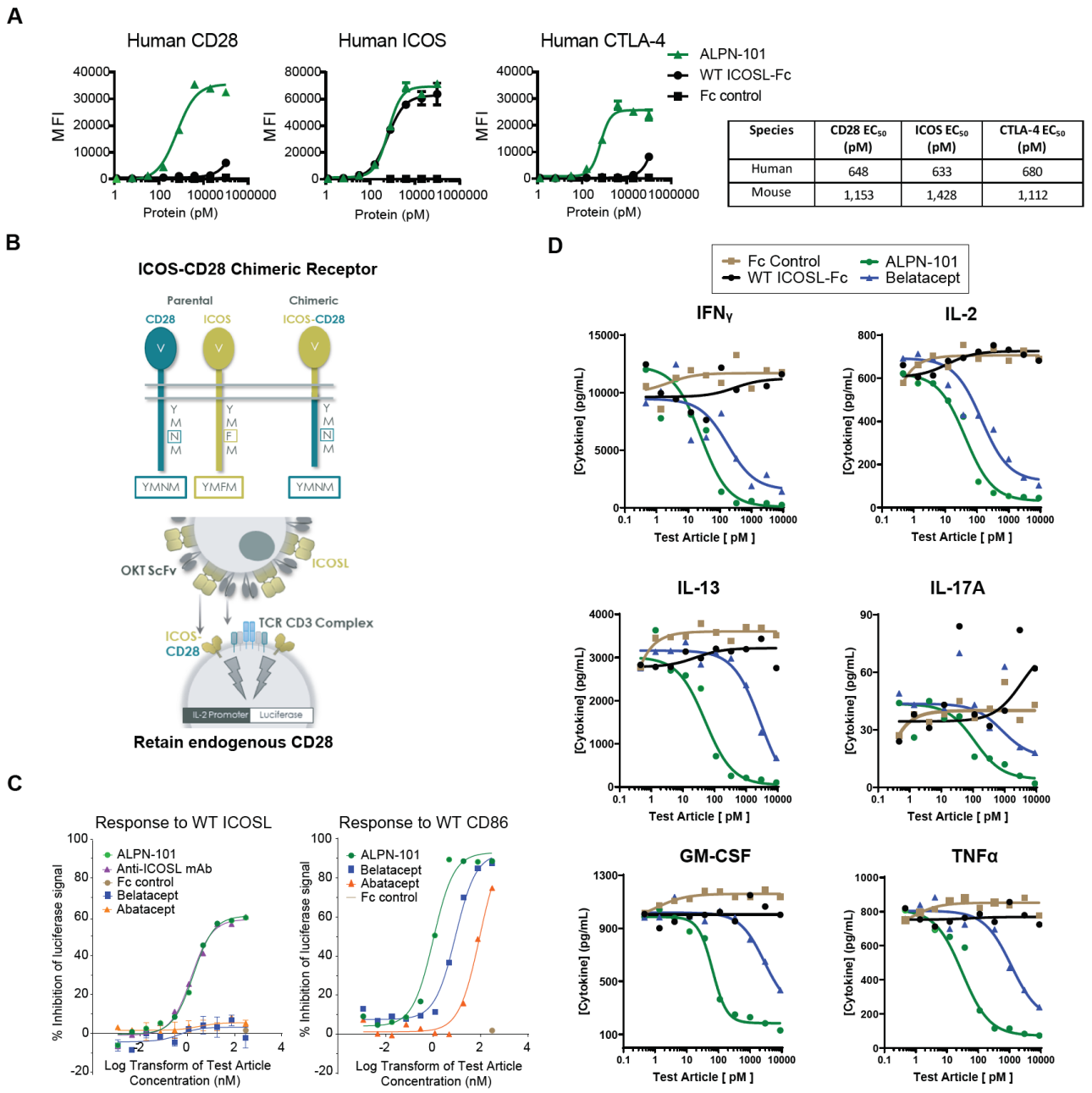

Fig. S13. ALPN-101 potently suppresses human T cell responses in vitro. (A) Flow cytometric analysis of ALPN-101, human wild-type (WT) ICOSL-Fc, and Fc control protein binding to Expi293 cells transfected with human CD28, ICOS, or CTLA-4, stained with a goat anti-human IgG-phycoerythrin (PE) detection antibody, and binding quantified by PE mean fluorescence intensity (MFI). Data are shown as mean ± SEM of triplicate wells and are representative of 3 independent experiments. **(B)** Diagram of the human Jurkat T cells expressing endogenous CD28, an IL-2-luciferase reporter gene, and a transfected chimeric ICOS/CD28 molecule that were used to evaluate ALPN-101 binding and blockade of both CD28- and ICOS-mediated signaling. **(C)** Inhibition of ICOSL-stimulated or CD86-stimulated luciferase signal by the indicated molecules. Cells described in B were stimulated with plate-bound WT ICOSL-Fc (left) or WT CD86-Fc (right) in the presence or absence of indicated concentrations of ALPN-101, belatacept, abatacept, anti-ICOSL mAb, or Fc control. The percent inhibition of the luciferase signal in the presence of various concentrations of the test molecules [defined as (1 – experimental value/mean value of Fc control wells) × 100] is plotted versus the log transform of test molecule concentration (nM). Data are shown as mean ± SEM of triplicate wells and are representative of 3 independent experiments. **(D)** Inhibition of cytokine secretion in a human mixed lymphocyte reaction (MLR) by ALPN-101. Concentrations of the indicated cytokines in the culture supernatants from MLR performed in the presence of the indicated concentrations of test compounds were measured using a Milliplex bead-based multiplex assay. Results shown are representative of at least 6 experiments with different donor pairs.

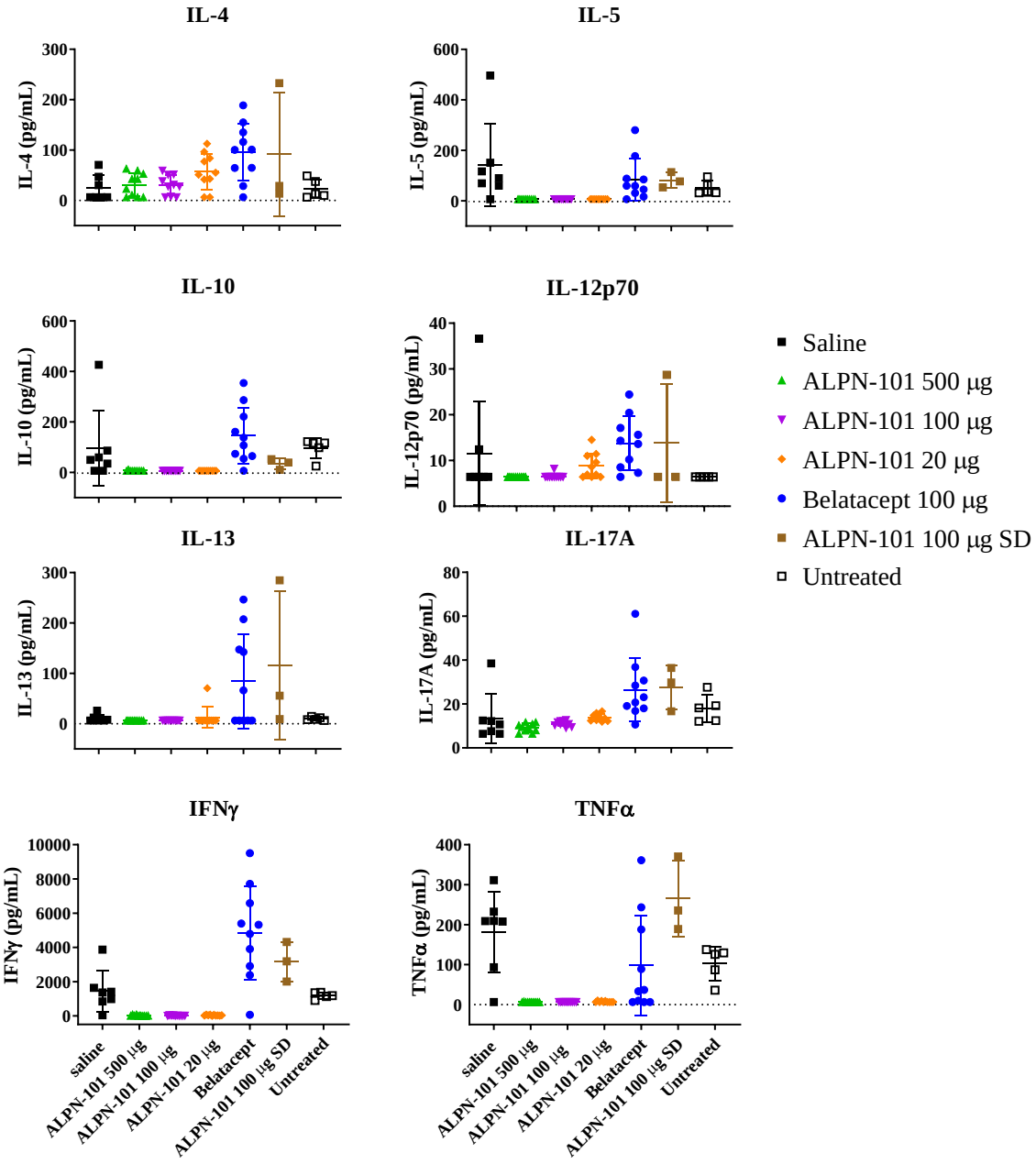

Fig. S14. Human cytokine concentrations measured in terminal serum collected from mice in all treatment groups in the human PBMC-NSG GvHD study. Serum samples were collected at termination (on various Study Days) from mice in each treatment group (unless mice were found dead before serum could be drawn) in the study described in **Fig. 3C-E**. Serum samples were diluted 1:2 and assayed with the human 12-plex Milliplex kit, as described in supplementary materials and methods. Other cytokines included in the assay panel but undetectable in the serum samples (and not included in the figure) were human IL-1β, IL-2, IL-6, and IL-8. LLOQ in the assays were 6.4 pg/mL. Statistical differences between groups are shown in table S8.

A

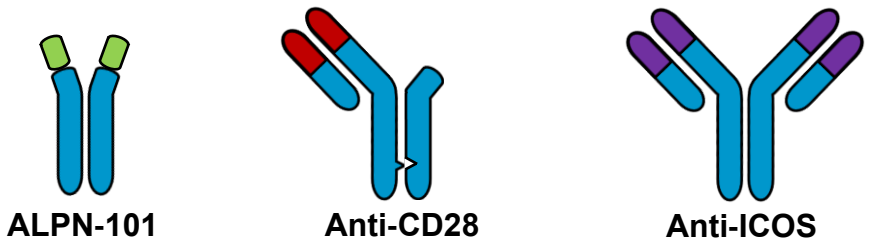

B

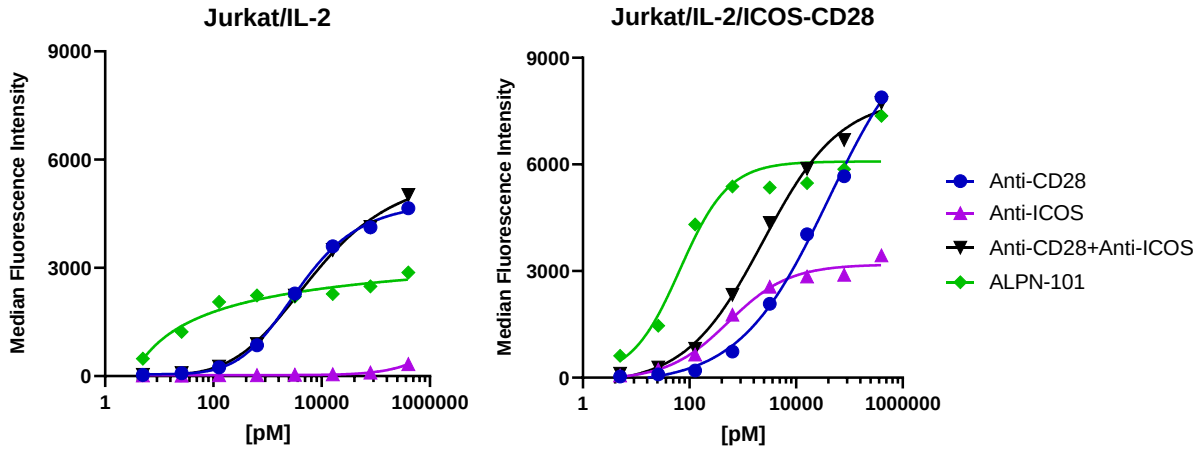

Cell Line	EC_{50} Values (pM)			
	Anti-CD28	**Anti-ICOS**	**Anti-CD28 + Anti-ICOS**	**ALPN-101**
Jurkat/IL-2	4859	-	5690	3932
Jurkat/IL-2/ICOS-CD28	41062	533	2402	66

Fig. S15. Evaluation of the binding of anti-CD28 and anti-ICOS antagonist Fc fusion proteins to Jurkat cells expressing endogenous CD28 or transfected chimeric ICOS-CD28 molecules. (**A**) Schematic representations of ALPN-101 and two comparator Fc fusion proteins produced at AIS for evaluation in the huPBMC-NSG GVHD model. The anti-CD28-Fc antagonist protein was engineered using a Fab domain derived from a CD28 antagonist antibody (red), fused with the same effectorless Fc tail contained within ALPN-101, as a 'knob-into-hole' heterodimeric Fc fusion protein. The anti-ICOS antagonist protein consists of the ICOS-binding Fab domains from vopratelimab (purple), also fused to the same effectorless Fc tail (blue). (**B**) Test molecules were evaluated at a range of concentrations by flow cytometry for their binding to Jurkat/IL-2 or Jurkat/IL-2/ICOS-CD28 cells using luciferase as the readout (described in fig. S13B) and EC_{50} values (pM) were calculated and summarized below the graphs.

A

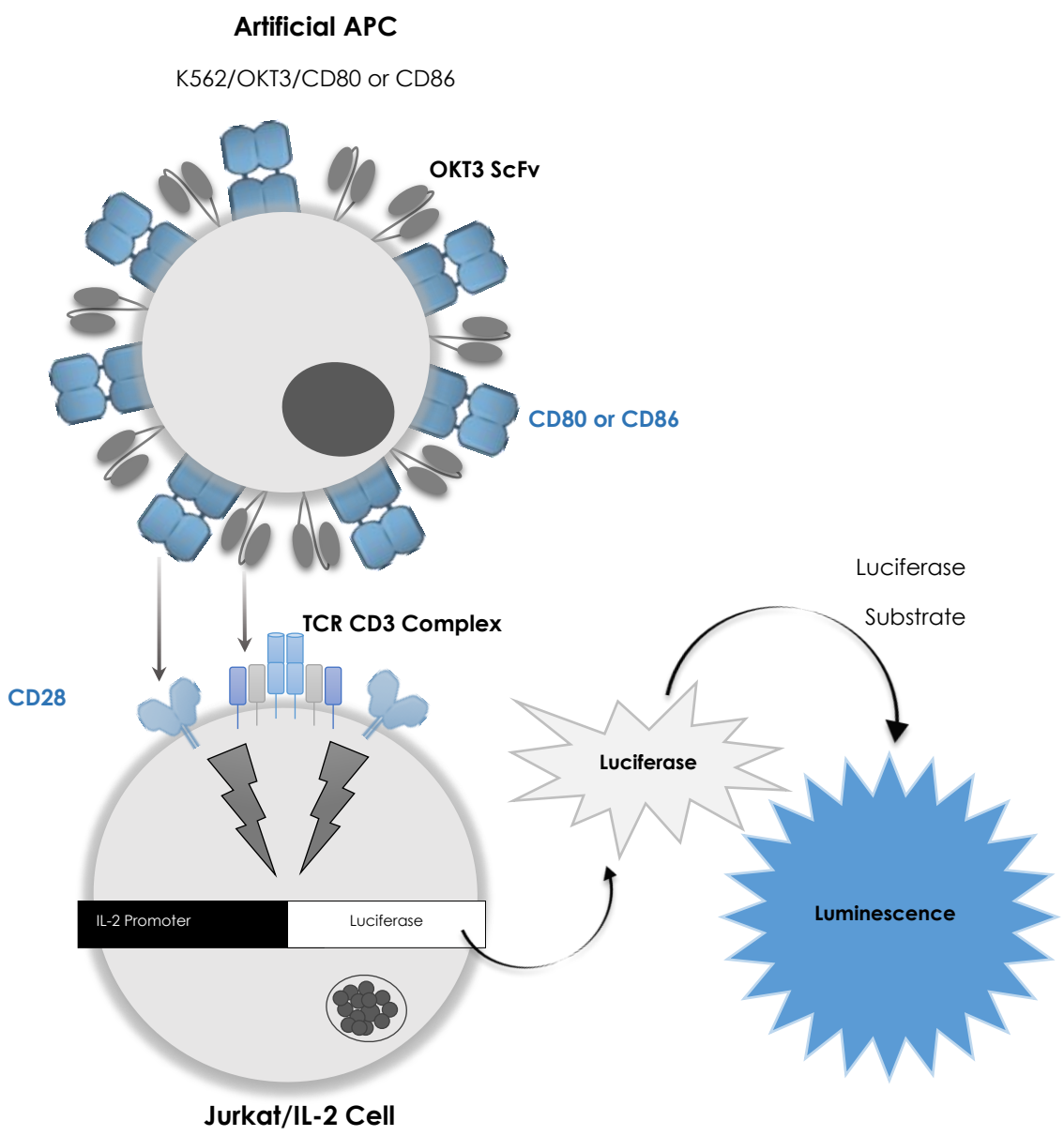
Artificial APC
K562/OKT3/CD80 or CD86
OKT3 ScFv
CD80 or CD86
TCR CD3 Complex
CD28
Luciferase
Substrate
Luciferase
Luminescence
IL-2 Promoter
Luciferase
Jurkat/IL-2 Cell

B

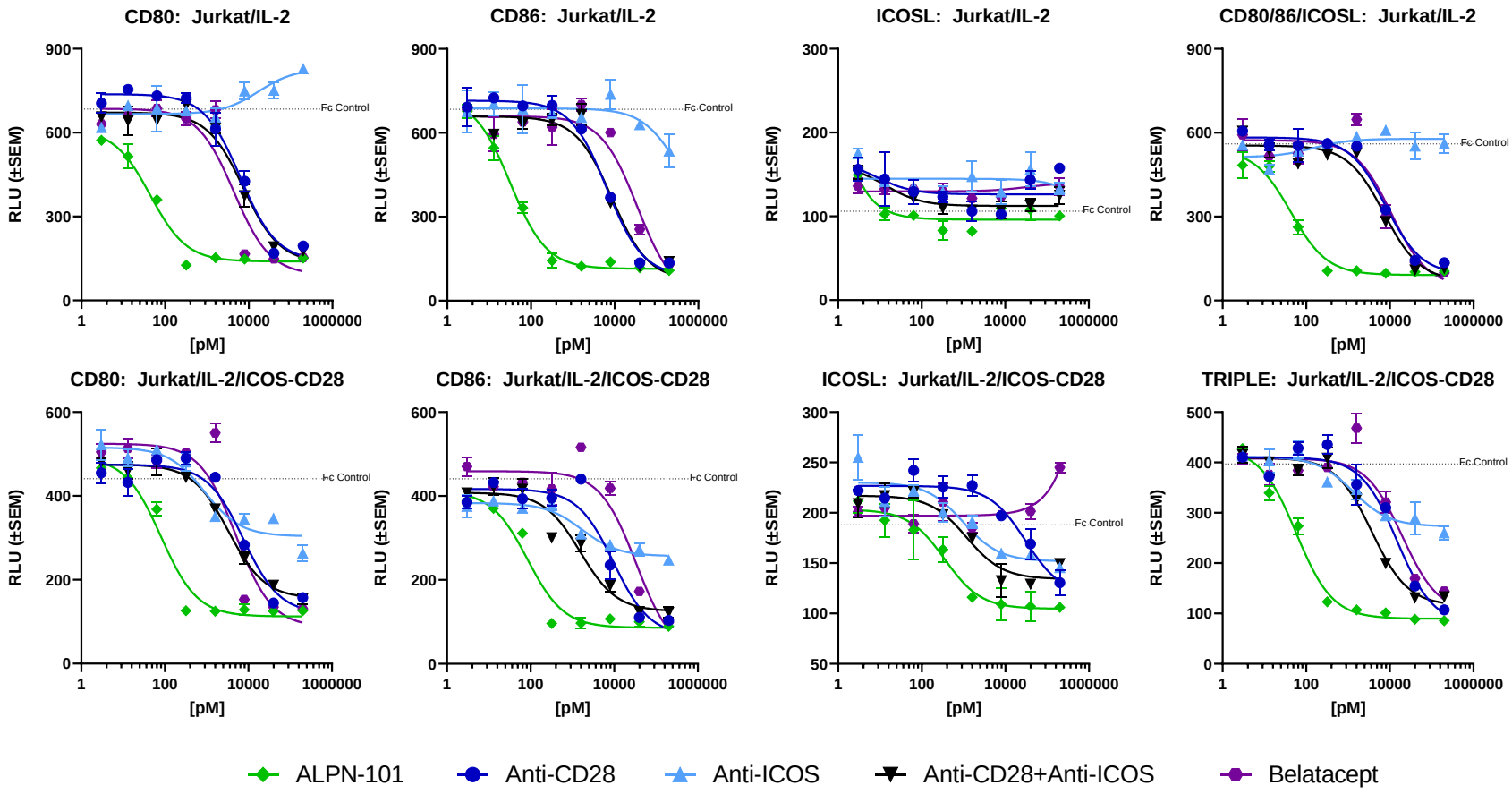
CD80: Jurkat/IL-2
CD86: Jurkat/IL-2
ICOSL: Jurkat/IL-2
CD80/86/ICOSL: Jurkat/IL-2
CD80: Jurkat/IL-2/ICOS-CD28
CD86: Jurkat/IL-2/ICOS-CD28
ICOSL: Jurkat/IL-2/ICOS-CD28
TRIPLE: Jurkat/IL-2/ICOS-CD28
RLU (±SEM)
[pM]
Fc Control
ALPN-101
Anti-CD28
Anti-ICOS
Anti-CD28+Anti-ICOS
Belatacept

Test Molecule	IC_{50} Values (pM) for Each Set of Artificial APC Stimulators and Responding Cell Types							
	aAPC: CD80		aAPC: CD86		aAPC: ICOSL		aAPC: CD80/CD86/ICOSL	
	Parental Jurkat	ICOS-CD28 Jurkat	Parental Jurkat	ICOS-CD28 Jurkat	Parental Jurkat	ICOS-CD28 Jurkat	Parental Jurkat	ICOS-CD28 Jurkat
Anti-CD28	6343	7643	6561	9649	-	30663	7993	14994
Anti-ICOS	17206	895	345680	1698	-	970	150	1341
Anti-CD28 + Anti-ICOS	7428	3359	8705	1545	-	1183	7283	3707
ALPN-101	44	81	32	84	-	352	43	58

Fig. S16. Blockade of CD28- or ICOS-mediated costimulation by ALPN-101, anti-CD28, anti-ICOS, combination anti-CD28$^+$ anti-ICOS, or belatacept. (**A**) Diagram of the assay used to evaluate blockade of various costimulatory pathways. Jurkat/IL-2 or Jurkat/IL-2/ICOS-CD28 cells (1.25×10^5 cells per well) were added to artificial APCs (aAPC, 2.5×10^4 cells per well) and titrated test molecules (200,000 – 3 pM). Test molecules (see fig. S15A) were ALPN-101, anti-CD28, anti-ICOS, anti-CD28 plus anti-ICOS, and belatacept. Fc control (dotted horizontal line) was added at 200,000 pM. (**B**) Shown are the results of blockade of CD80/CD28-mediated costimulation, CD86/CD28-mediated costimulation, ICOSL/ICOS-mediated costimulation, and of all three pathways (CD80, CD86, ICOSL) for Jurkat/IL-2 (upper row) and Jurkat/IL-2/ICOS-CD28 cells (lower row). IC_{50} values (pM) for each set of conditions are provided in the last part of the figure. Data shown represent an average ± SEM of triplicate wells for each condition and are representative of results obtained in 3 separate experiments.

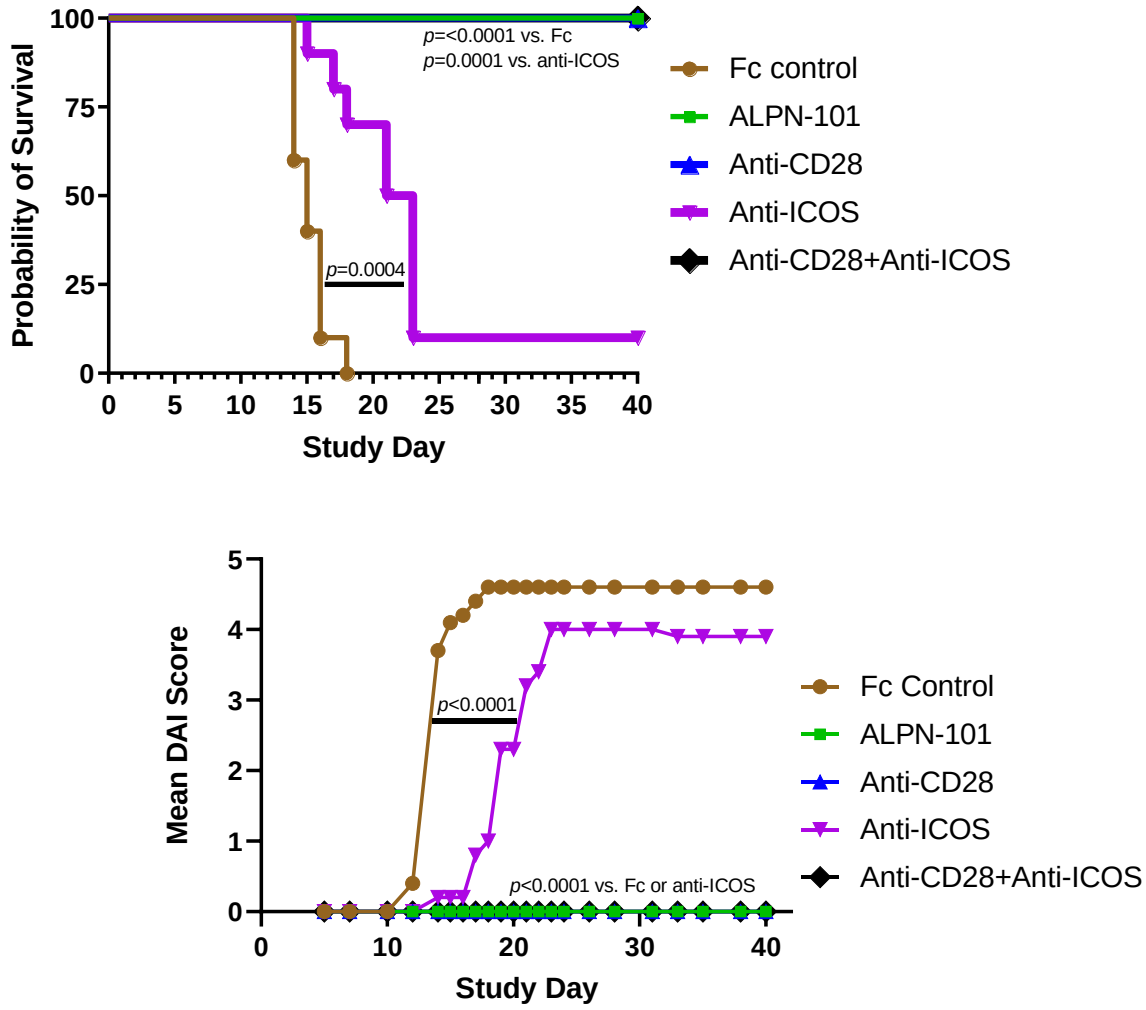

Fig. S17. Dual blockade of CD28 and ICOS or CD28 alone prevents GVHD in the human PBMC-NSG model. On Day –1, female NSG mice (8/group) were irradiated (100 cGy) and subcutaneously administered 10 mg human gamma globulin. On Day 0, mice received 1×10^7 human PBMC intravenously. Intraperitoneal dosing began on Day 0 and continued 3× weekly through Day 18 with molar-matched doses of test molecules: 75 µg Fc control (the same Fc contained in all test molecules), 100 µg ALPN-101, 125 µg anti-CD28, 180 µg anti-ICOS, or a combination of 125 µg anti-CD28 + 180 µg anti-ICOS. The study was terminated on Day 40; endpoints included survival and disease activity index (DAI), which included body weight loss as one component. Statistical significance for survival data was assessed by log-rank (Mantel-Cox) test: $p<0.0001$ for ALPN-101, anti-CD28, or combination anti-CD28+anti-ICOS versus Fc control; $p=0.0001$ for ALPN-101, anti-CD28, or combination anti-CD28+anti-ICOS versus anti-ICOS; $p=0.0004$ for anti-ICOS versus Fc control. For DAI, statistical significance was assessed by two-way repeated-measures ANOVA for treatment effect; $p<0.0001$ for ALPN-101, anti-CD28, anti-ICOS, and combination anti-CD28+anti-ICOS versus Fc control. $p<0.0001$ for ALPN-101, anti-CD28 and combination anti-CD28+anti-ICOS versus anti-ICOS.

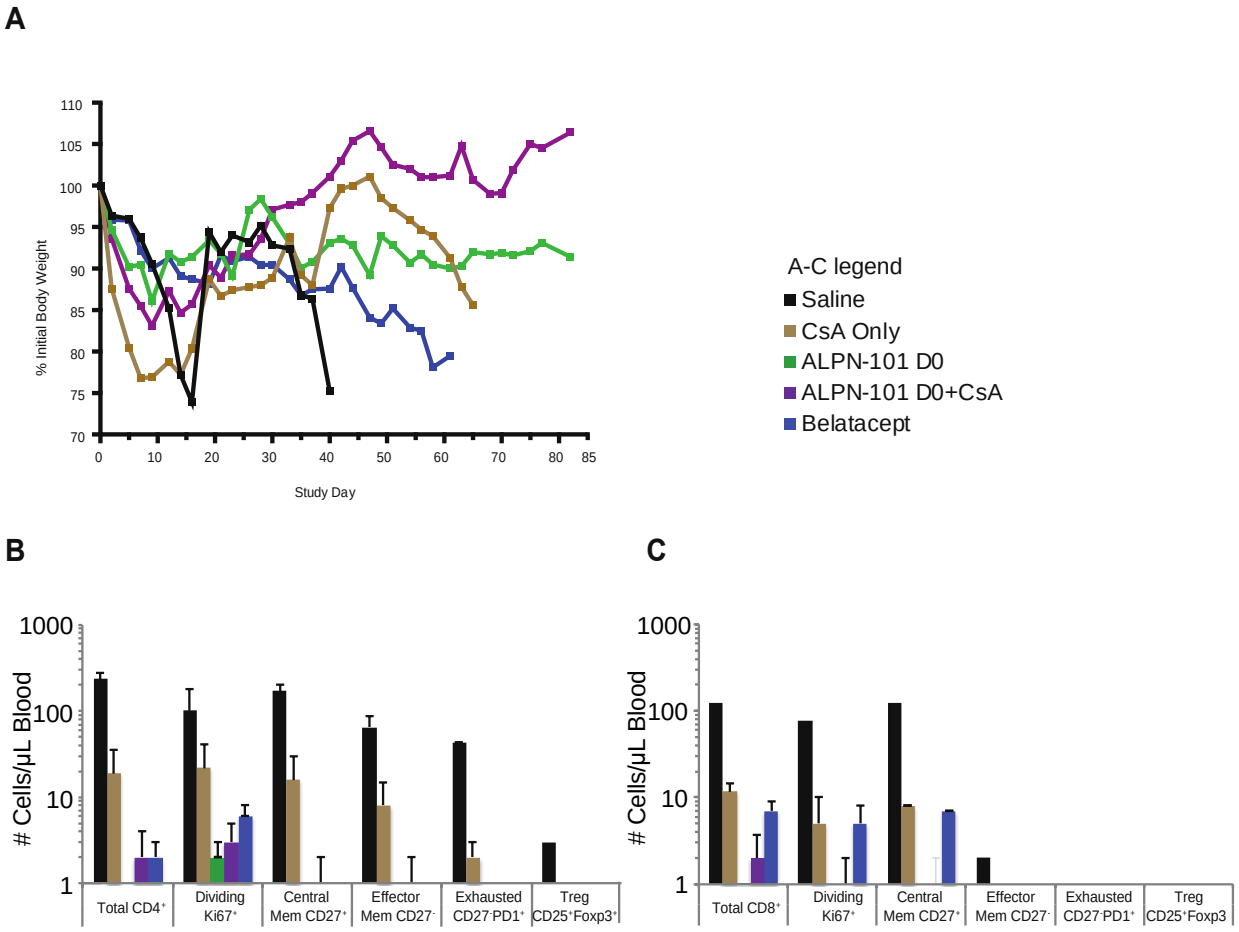

Fig. S18. Percent change in BW and flow analysis of T cells in blood from human PBMC-NSG mice treated with ALPN-101 with or without CsA. (**A**) Mice were weighed daily to track body weight loss throughout the study described in **Fig. 4D**. The mean % of baseline BW is plotted vs. Study Day for all treatment groups. (**B-C**) Blood was collected at Day 15 from all surviving mice in the study shown in **Fig. 4D** and engrafted human $CD45^+$ cells were characterized by flow cytometry using detection reagents specific for CD3, CD4, CD8, CD14, CD16, CD20, CD25, CD27, CD28, CD45RA, CD56, CD95, FoxP3, ICOS, CCR7, Ki67, and PD-1. The mean and standard deviation from the mean of the number of cells per µL blood with each indicated phenotype for the gated $CD4^+$ (B) and $CD8^+$ (C) T cell subsets are plotted.

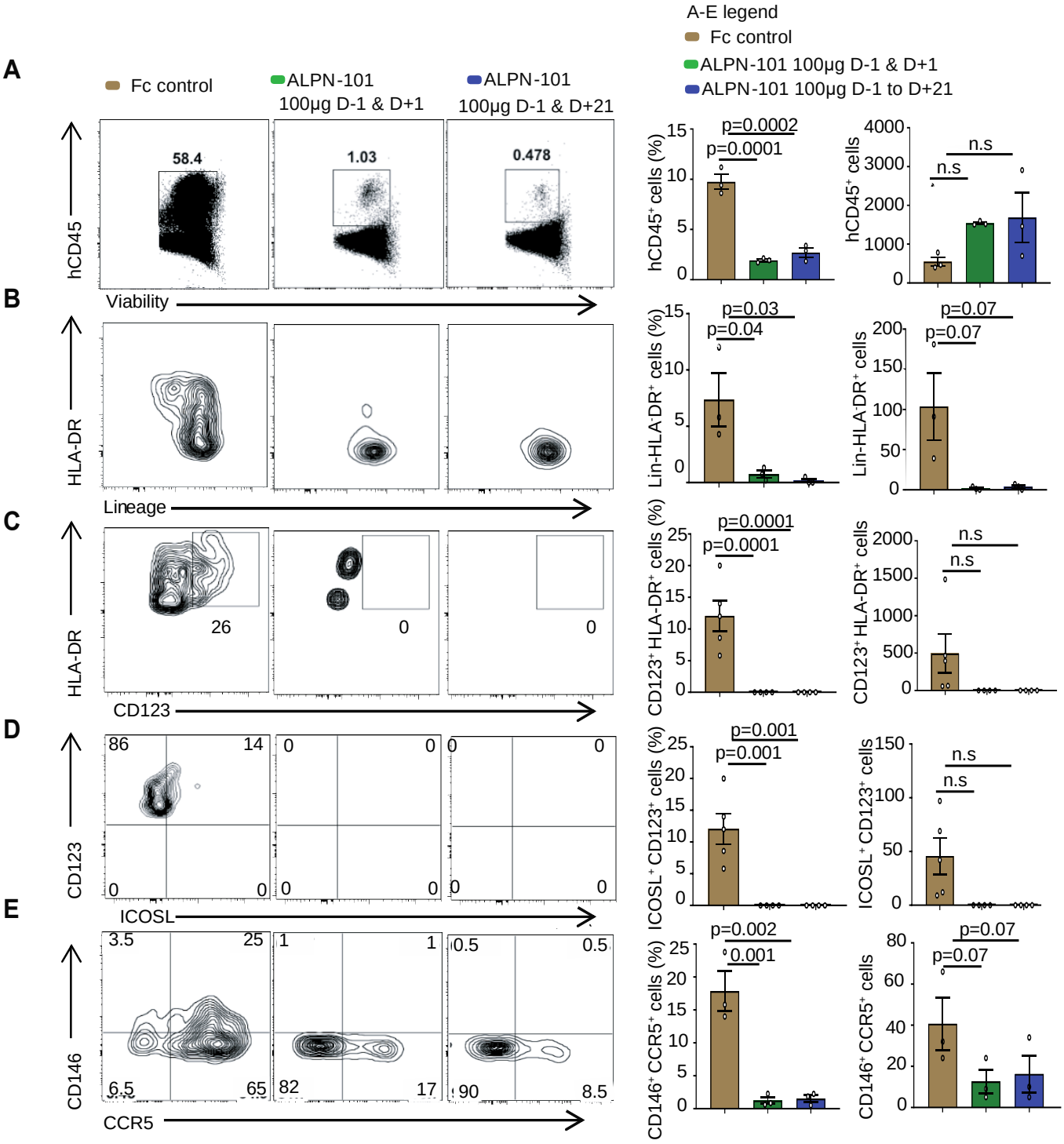

Fig. S19. Frequency and absolute counts of human infiltrating splenic cells in the peri-transplant and prophylactic human PBMC-NSG study. (A) Human hematopoietic cell engraftment, **(B)** Lineage$^-$ HLA-DR$^+$ total dendritic cells, **(C)** HLA-DR$^+$CD123$^+$ pDCs, **(D)** ICOSL$^+$ pDCs, and **(E)** CD146$^+$CCR5$^+$ T cells. NSG mice were analyzed at Day 14 after HCT comparing the Fc control and ALPN-101–treated groups (2 doses versus 12 doses), n=3 in each group. Data are shown as mean ± SEM and statistical significance determined by ANOVA with Bonferroni's correction for multiple comparisons.

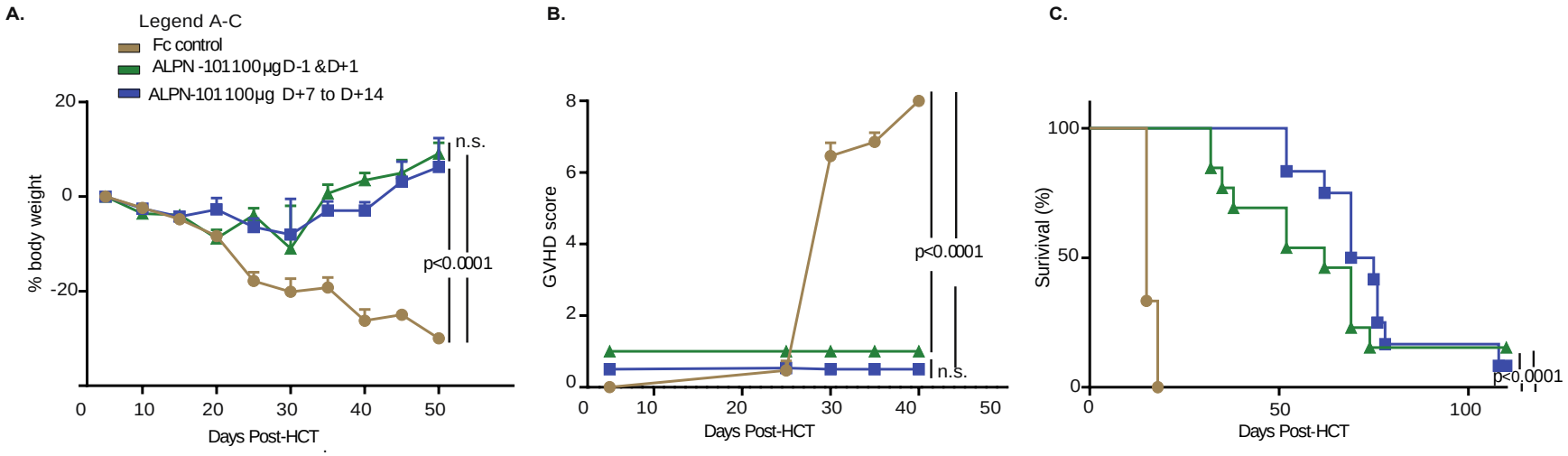

Fig. S20. Prophylactic blockade of ICOS/CD28 on donor pDCs using ALPN-101 in an aggressive xenogeneic GVHD model. (**A**) Body weight loss, (**B**) GVHD disease score, and (**C**) survival of NSG irradiated with 350 cGy at Day –1, then transplanted with 5×10^6 human PBMC at Day +1. Mice were treated every other day with Fc control or 100 µg of ALPN-101 from Day –1 to Day +21 (12 doses total) or 100 µg of ALPN-101 on Day –1 and Day +1 (2 doses total); n=10 in all groups. Data are shown as mean ± SEM, and statistical significance was determined by ANOVA with Bonferroni's correction for multiple comparisons; a log-rank test was used for survival analysis.

Table S1. Characteristics of the study patients. n/a=not applicable

	GI-GVHD	No GVHD	Non-GVHD Enteritis	Skin GVHD	
Total, n = 156	**n = 64**	**n = 39**	**n = 22**	**n = 31**	**p-value**
Median age	47 (0-66)	48 (2-67)	47 (5-65)	52 (1-65)	0.54
Disease, %					
Malignant	97 (n = 62)	95 (n = 37)	96 (n = 21)	97 (n = 30)	0.32
Other	3 (n = 2)	5 (n = 2)	4 (n = 1)	3 (n = 1)	
Disease status at transplantation, %					
Low/intermediate risk	59 (n = 38)	64 (n = 25)	59 (n = 13)	68 (n = 21)	0.77
High risk	41 (n = 26)	36 (n = 14)	41 (n = 9)	32 (n = 10)	
Donor type, %					
Related donor	38 (n = 24)	64 (n = 25)	59 (n = 13)	42 (n = 13)	0.04
Unrelated donor	62 (n = 40)	36 (n = 14)	41 (n = 9)	58 (n = 18)	
Donor match, %					
Matched donor	75 (n = 48)	85 (n = 33)	86 (n = 19)	84 (n = 26)	0.49
Mismatched donor	25 (n = 16)	15 (n = 6)	14 (n = 3)	16 (n = 5)	
Conditioning regimen intensity, %					
High intensity	78 (n = 50)	85 (n = 33)	91 (n = 20)	77 (n = 24)	0.50
Reduced intensity	22 (n = 14)	15 (n = 6)	9 (n = 2)	23 (n = 7)	
Median (range) of onset/matched time after HCT	29 (11-92)	29 (14-131)	33 (14-78)	29 (7-87)	0.38
Stage of GVHD at onset, %					
Skin Stage 1-2	34 (n = 22)	0 (n = 0)	0 (n = 0)	77 (n = 24)	n/a
Stage 3-4	17 (n = 11)	0 (n = 0)	0 (n = 0)	23 (n = 7)	
GI Stage 1	64 (n = 41)	0 (n = 0)	0 (n = 0)	0 (n = 0)	n/a
Stage 2-4	36 (n = 23)	0 (n = 0)	0 (n = 0)	0 (n = 0)	

Table S2. Causes of overall mortality in patients with GVHD symptoms (*n* = 117). Results are presented in frequency with (%) rounded to the nearest whole number. aGVHD- acute graft versus host disease, cGVHD – chronic graft versus host disease.

Death due to recurrence or persistence of primary disease	**27% (n=32)**
Non-relapse mortality	**33% (n=39)**
Death by aGVHD	15% (n=17)
Death by cGVHD	6% (n=8)
Death by hemorrhage	2% (n=2)
Death by idiopathic pneumonia syndrome	1% (n=1)
Death by sinusoidal obstructive syndrome	2% (n=2)
Death by infection	2% (n=2)
Death by cardiac toxicity	1% (n=1)
Death by renal failure	1% (n=1)
Death by multiple organ failure	1% (n=1)
Death by secondary malignancy	1% (n=1)
Unknown cause of death	3% (n =3)

Table S3. Relative affinities of ALPN-101 to human CD28, ICOS, and CTLA-4 measured by BLI analysis. The association (k_a) and disassociation (k_d) rates for ALPN-101 binding to recombinant monomeric CD28:His, ICOS:His, and CTLA-4:His were determined by biolayer interferometry analysis as described in supplementary materials and methods. Both pM and M versions of the K_D are reported, along with k_a, k_d, and their respective errors and %CV. The error of each calculated value is reported to give confidence to the values reported and ideally should be less than 10%. Full R^2 is also reported to give confidence to the global fit of a 1:1 model; ideally, this value would be as close to 1 as possible. Results shown are from 3 independent experiments.

Sample	K_D (pM)	K_D (M)	% CV	K_D Error	% CV	k_a(1/Ms)	% CV	k_a Error	% CV	k_d(1/s)	% CV	k_d Error	% CV	Full R^2	% CV
ICOS	306	3.06E-10	11.8	<1.0E-12	n/a	2.31E+05	4.85	1.96E+02	14.2	7.09E-05	16.6	<1.0E-07	n/a	0.997	0.06
CD28	1257	1.26E-09	23.2	3.4E-12	22.7	1.21E+05	13.4	1.64E+02	13.1	1.92E-04	22.6	3.08E-07	14.5	0.996	0.11
CTLA-4	471	4.71E-10	11.3	1.42E-12	21.7	1.32E+05	1.56	178.5667	21.6	6.22E-05	11.3	1.67E-07	22.4	0.996	0.16

Table S4. Summary of protocols used for the human PBMC-NSG GVHD studies. All protocols included subcutaneous injection of human IgG on Day 0.

Figures	Location of study	Source of NSG mice	Irradiation source (dose)	# Human PBMCs injected	Length of study
3C-F, S14-16	JAX	JAX	X-ray (100 cGy)	10×10^6	42 days
4A-C	JAX	JAX	X-ray (100 cGy)	10×10^6	55 days
4D, S18	U Minn	JAX/bred at U Minn	X-ray (180 cGy)	10×10^6	84 days
S17	JAX	JAX	X-ray (100 cGy)	10×10^6	40 days
5D-G	IU	IU In Vivo Core	^{137}C (300 cGy)	3.5×10^6	60 days
S19	IU	IU In Vivo Core	^{137}C (300 cGy)	3.5×10^6	60 days
S20	IU	IU In Vivo Core	^{137}C (350 cGy)	5×10^6	110 days
6A-G	IU	IU In Vivo Core	^{137}C (350 cGy)	5×10^6	120 days
6I-K	IU	IU In Vivo Core	^{137}C (300 cGy)	4×10^6 (and 1×10^6 MOLM-14-EGFP cells)	42 days

Table S5. Final circulating T cell counts and statistical analysis for the GVHD survival, DAI, and BW loss data.

A Final circulating human T cell counts in surviving mice on Day 42 (Fig. 3C-D)

Treatment Group	Total T Cell Number on Day 42 (in surviving individual mice), cells/mL blood									
ALPN 101 500 µg	3670	11160	7750	12640	35680	56540	89330	59900	52200	12570
ALPN 101 100 µg	260670	9850	32000	2430	1540	118840	5500	23540	36960	160
ALPN 101 20 µg	11340	28790	171600	55360	18220	4710	39760	104760	2720	15780
Belatacept 100 µg	12477570	14540	728470	2304640						

B Survival curves (Fig. 3C, left)

TEST ARTICLE	Saline	ALPN-101 TIW x 4 (20 µg)	ALPN-101 TIW x 4 (100 µg)	ALPN-101 TIW x 4 (500 µg)	Belatacept TIW x 4 (100 µg)	ALPN-101 single dose (100 µg)
Saline		*p*<0.0001	*p*<0.0001	*p*<0.0001	*p*<0.0001	*p*<0.0001
ALPN-101 TIW x 4 (20 µg)	*p* <0.0001		ns	ns	*p*<0.01	*p*<0.001
ALPN-101 TIW x 4 (100 µg)	*p*<0.0001	ns		ns	*p*<0.01	*p*<0.001
ALPN-101 TIW x 4 (500 µg)	*p*<0.0001	ns	ns		*p*<0.01	*p*<0.001
Belatacept TIW x 4	*p*<0.0001	*p*<0.01	*p*<0.01	*p*<0.01		*p*=0.457 (ns)
ALPN-101 single dose	*p*<0.0001	*p*<0.001	*p*<0.001	*p*<0.001	*p*=0.457 (ns)	

Statistical differences in survival proportions between groups for the data presented in **Fig. 3A** were analyzed using the Mantel-Cox (log-rank) test: p<0.05 considered significant; ns= not significant. TIW = three times/week.

C DAI scores (Fig. 3C, middle)

TEST ARTICLE	Saline	ALPN-101 TIW x 4 (20 µg)	ALPN-101 TIW x 4 (100 µg)	ALPN-101 TIW x 4 (500 µg)	Belatacept TIW x 4 (100 µg)	ALPN-101 single dose (100 µg)
Saline		$p<0.0001$	$p<0.0001$	$p<0.0001$	$p=0.0086$	$p<0.0001$
ALPN-101 TIW x 4 (20 µg)	$p<0.0001$		$p=0.5127$	$p=0.0155$	$p=0.0113$	$p=0.0038$
ALPN-101 TIW x 4 (100 µg)	$p<0.0001$	$p=0.5127$		$p=0.0138$	$p=0.0635$	$p=0.0436$
ALPN-101 TIW x 4 (500 µg)	$p<0.0001$	$p=0.0155$	$p=0.0138$		$p=0.0022$	$p<0.0001$
Belatacept TIW x 4	$p=0.0086$	$p=0.0113$	$p=0.0635$	$p<0.0001$		$p=0.3625$ (ns)
ALPN-101 single dose	$p<0.0001$	$p=0.0038$	$p=0.0436$	$p<0.0001$	$p=0.3625$	

Statistical differences in DAI scores between groups for the data presented in **Fig. 3B** were analyzed by 2-way repeated measures ANOVA for treatment effect: p<0.05 considered significant; ns= not significant. TIW = three times/week.

D Terminal BW loss (Fig. 3C, right)

TEST ARTICLE	Saline	ALPN-101 TIW x 4 (20 µg)	ALPN-101 TIW x 4 (100 µg)	ALPN-101 TIW x 4 (500 µg)	Belatacept TIW x 4 (100 µg)	ALPN-101 single dose (100 µg)
Saline		$p<0.0001$	$p<0.0001$	$p<0.0001$	$p>0.9999$	$p>0.9999$
ALPN-101 TIW x 4 (20 µg)	$p<0.0001$		$p>0.9999$	$p>0.9999$	$p=0.0078$	$p=0.0002$
ALPN-101 TIW x 4 (100 µg)	$p<0.0001$	$p>0.9999$		$p>0.9999$	$p=0.0008$	$p<0.0001$
ALPN-101 TIW x 4 (500 µg)	$p<0.0001$	$p>0.9999$	$p>0.9999$		$p=0.0001$	$p<0.0001$
Belatacept TIW x 4	$p>0.9999$	$p=0.0078$	$p=0.0008$	$p=0.0001$		$p>0.9999$
ALPN-101 single dose (100 µg)	$p>0.9999$	$p=0.0002$	$p<0.0001$	$p<0.0001$	$p>0.9999$	

Statistical differences in terminal % body weight loss between groups for the data presented in **fig. S14** were analyzed by 1-way ANOVA with Bonferroni correction: p<0.05 considered significant; ns= not significant. TIW = three times/week.

Table S6. Statistical analysis of terminal serum human cytokine concentrations in mice treated with repeat 100-µg doses of ALPN-101 or belatacept, or a single 100-µg dose of ALPN-101. Terminal serum cytokine data shown in fig. S14, from the GVHD study shown in **Fig. 3C-F**, were analyzed for statistically significant differences between groups using an unpaired parametric t-test. Values of $p<0.05$ are considered significant; ns = non-significant.

IL-4	**ALPN-101 (100 µg)**	**Belatacept (100 µg)**	**ALPN-101 single dose (100 µg)**
Saline	ns	$p<0.01$	ns
ALPN-101 (100 µg)	-	$p<0.01$	ns
Belatacept (100 µg)	$p<0.01$	-	ns

IL-5	**ALPN-101 (100 µg)**	**Belatacept (100 µg)**	**ALPN-101 single dose (100 µg)**
Saline	$p<0.05$	ns	ns
ALPN-101 (100 µg)	-	$p<0.01$	$p<0.0001$
Belatacept (100 µg)	$p<0.01$	-	ns

IL-10	**ALPN-101 (100 µg)**	**Belatacept (100 µg)**	**ALPN-101 single dose (100 µg)**
Saline	ns	ns	ns
ALPN-101 (100 µg)	-	$p<.001$	$p<.001$
Belatacept (100 µg)	$p<.001$	-	ns

IL-12 p70	**ALPN-101 (100 µg)**	**Belatacept (100 µg)**	**ALPN-101 single dose (100 µg)**
Saline	ns	ns	ns
ALPN-101 (100 µg)	-	$p<0.01$	ns
Belatacept (100 µg)	$p<0.01$	-	ns

IL-13	**ALPN-101 (100 µg)**	**Belatacept (100 µg)**	**ALPN-101 single dose (100 µg)**
Saline	ns	ns	ns
ALPN-101 (100 µg)	-	$p<0.05$	$p<0.05$
Belatacept (100 µg)	$p<0.05$	-	ns

IL-17A	**ALPN-101 (100 µg)**	**Belatacept (100 µg)**	**ALPN-101 single dose (100 µg)**
Saline	ns	ns	ns
ALPN-101 (100 µg)	-	$p<0.01$	$p=0.0001$
Belatacept (100 µg)	$p<0.01$	-	ns

IFNγ	**ALPN-101 (100 µg)**	**Belatacept (100 µg)**	**ALPN-101 single dose (100 µg)**
Saline	$p<0.01$	$p<0.01$	ns
ALPN-101 (100 µg)	-	$p<0.0001$	$p<0.0001$
Belatacept (100 µg)	$p<0.0001$	-	ns

TNFα	**ALPN-101 (100 µg)**	**Belatacept (100 µg)**	**ALPN-101 single dose (100 µg)**
Saline	$p<0.0001$	ns	ns
ALPN-101 (100 µg)	-	$p<0.05$	$p<0.0001$
Belatacept (100 µg)	$p<0.05$	-	ns

Table S7. Summary of statistical significance for survival between treatment groups in the human PBMC-NSG GVHD study. Statistical differences in survival proportions between groups (**Fig. 4A**) were analyzed using the Mann-Whitney (log-rank) test. Values of $p<0.05$ are considered significant; ns = not significant.

TEST ARTICLE	**Saline**	**Belatacept RD**	**Belatacept SD**	**ALPN-101 RD**	**ALPN-101 SD**
Saline		$p<0.0001$	$p=0.0189$	$p<0.0001$	$p=0.0022$
Belatacept RD	$p<0.0001$		$p<0.0001$	$p=0.0667$ (ns)	$p=0.7646$ (ns)
Belatacept SD	$p=0.0189$	$p<0.0001$		$p=0.0014$	$p=0.0043$
ALPN-101 RD	$p<0.0001$	$p=0.0667$ (ns)	$p=0.0014$		$p=0.2398$ (ns)
ALPN-101 SD	$p=0.0022$	$p=0.7646$ (ns)	$p=0.0043$	$p=0.2398$ (ns)	

Statistical differences in survival proportions between groups for the data presented in **Fig. 4A** were analyzed using the Mann-Whitney (log-rank) test: $p<0.05$ considered significant; ns= not significant. RD = repeat dose, SD = single dose.

Table S8. Additional correlation analyses of the flow cytometric data from the human PBMC-NSG GVHD study. Correlation values for the study shown in **Fig. 4A-C.** Negative R^2 values denote an inverse correlation.

		Correlation Coefficient (R^2 Value) for % Cells Positive for Marker versus Each Endpoint		
Marker	**T Cell Subset**	**DAI**	**% Change in BW**	**Survival Day**
ICOS	**$CD4^+$**	0.49	-0.68	-0.83
	$CD8^+$	0.75	-0.78	-0.76
CD28	**$CD4^+$**	0.38	-0.39	-0.29
	$CD8^+$	0.34	-0.50	-0.74
PD-1	**$CD4^+$**	0.03	-0.05	-0.01
	$CD8^+$	0.08	-0.03	0.02

Table S9. Summary of statistical significance for survival between treatment groups in the human PBMC-NSG GVHD study. Statistical differences in survival proportions between groups (**Fig. 4D**) were analyzed using the Mantel-Cox (log-rank) test (upper table) and Gehan-Breslow-Wilcoxon test (lower table). Values of $p<0.05$ are considered significant; ns = not significant.

Mantel-Cox	**PBS**	**CsA only**	**ALPN-101 D0**	**ALPN-101 D0 + CsA**	**Belatacept**
PBS					
CsA only	0.8878 (ns)				
ALPN-101 D0	0.0002	0.0023			
ALPN-101 D0 + CsA	0.0005	0.0029	0.8806 (ns)		
Belatacept	0.0021	0.1459 (ns)	0.04	0.0183	
Gehan-Breslow-Wilcoxon	**PBS**	**CsA only**	**ALPN-101 D0**	**ALPN-101 D0 + CsA**	**Belatacept**
PBS					
CsA only	0.5691 (ns)				
ALPN-101 D0	0.0002	0.0012			
ALPN-101 D0 + CsA	0.0007	0.0026	0.9003 (ns)		
Belatacept	0.0004	0.0063	0.1003 (ns)	0.097 (ns)	